In-silico Investigation of Antitrypanosomal Phytochemicals from Nigerian Medicinal Plants

William N. Setzer[1]*, Ifedayo V. Ogungbe[1,2]

1 Department of Chemistry, University of Alabama in Huntsville, Huntsville, Alabama, United States of America, 2 Department of Metabolism and Aging, Scripps Research Institute, Jupiter, Florida, United States of America

Abstract

Background: Human African trypanosomiasis (HAT), a parasitic protozoal disease, is caused primarily by two subspecies of *Trypanosoma brucei*. HAT is a re-emerging disease and currently threatens millions of people in sub-Saharan Africa. Many affected people live in remote areas with limited access to health services and, therefore, rely on traditional herbal medicines for treatment.

Methods: A molecular docking study has been carried out on phytochemical agents that have been previously isolated and characterized from Nigerian medicinal plants, either known to be used ethnopharmacologically to treat parasitic infections or known to have *in-vitro* antitrypanosomal activity. A total of 386 compounds from 19 species of medicinal plants were investigated using *in-silico* molecular docking with validated *Trypanosoma brucei* protein targets that were available from the Protein Data Bank (PDB): Adenosine kinase (TbAK), pteridine reductase 1 (TbPTR1), dihydrofolate reductase (TbDHFR), trypanothione reductase (TbTR), cathepsin B (TbCatB), heat shock protein 90 (TbHSP90), sterol 14α-demethylase (TbCYP51), nucleoside hydrolase (TbNH), triose phosphate isomerase (TbTIM), nucleoside 2-deoxyribosyltransferase (TbNDRT), UDP-galactose 4′ epimerase (TbUDPGE), and ornithine decarboxylase (TbODC).

Results: This study revealed that triterpenoid and steroid ligands were largely selective for sterol 14α-demethylase; anthraquinones, xanthones, and berberine alkaloids docked strongly to pteridine reductase 1 (TbPTR1); chromenes, pyrazole and pyridine alkaloids preferred docking to triose phosphate isomerase (TbTIM); and numerous indole alkaloids showed notable docking energies with UDP-galactose 4′ epimerase (TbUDPGE). Polyphenolic compounds such as flavonoid gallates or flavonoid glycosides tended to be promiscuous docking agents, giving strong docking energies with most proteins.

Conclusions: This *in-silico* molecular docking study has identified potential biomolecular targets of phytochemical components of antitrypanosomal plants and has determined which phytochemical classes and structural manifolds likely target trypanosomal enzymes. The results could provide the framework for synthetic modification of bioactive phytochemicals, *de novo* synthesis of structural motifs, and lead to further phytochemical investigations.

Introduction

Human African trypanosomiasis (HAT), also known as *sleeping sickness*, is caused by the single-celled kinetoplastid parasites, *Trypanosoma brucei*, which are transmitted to humans by infected tsetse flies (*Glossina* spp.). Two sub-species of *T. brucei* (*rhodesiense* and *gambiense*) cause the two different forms of the disease. *T. b. rhodesiense* is found in southern and eastern Africa while *T. b. gambiense* is found in the western, central and some parts of eastern Africa. *T. b. gambiense* now accounts for about 90% of all reported cases of sleeping sickness. A third subspecies, *T. b. brucei*, does not cause HAT because of its susceptibility to lysis by human apolipoprotein L1 [1].

Current chemotherapies of HAT are directed either to the early or late stages of the disease. All the clinically available HAT chemotherapeutic drugs have been noted to be ineffective, and they also have severe side-effects. The only drug candidate in clinical trials for the treatment of HAT is the nitroimidazole fexinidazole. Fexinidazole is currently in clinical study for the treatment of the late stage form of HAT [2,3]. It is worth noting that the number of reported cases of HAT fell in the past decade, and it has also been suggested that a possible elimination of the disease might be in sight [4]. This is a very delightful development for this "neglected" tropical disease, and it is our hope that continued research into new and effective chemotherapy against HAT remains an integral part of public health initiatives in endemic communities.

Medicinal plants from Nigeria's lush rainforest, as well as her very diverse montane and savanna vegetation, continue to play a vital role in her healthcare system. For tens of millions of Nigerians, indigenous traditional medicine is the major – and sometimes the only – access to pharmacological agents [5]. There have been several published reports on the biological activity of

Author Summary

Traditional herbal medicine continues to play a key role in health, particularly in remote areas with limited access to "modern medicines". Many plants are used in traditional Nigerian medicine to treat parasitic diseases. While many of these plants have shown notable activity against parasitic protozoa, in most cases the mode of activity is not known. That is, it is not known what biochemical entities are being targeted by the plant chemical constituents. In this work, we have carried out molecular docking studies of known phytochemicals from Nigerian medicinal plants used to treat human African trypanosomiasis (sleeping sickness) with known biochemical targets in the *Trypanosoma brucei* parasite. The goals of this study were to identify the protein targets that the medicinal plants are affecting and to discern general trends in protein target selectivity for phytochemical classes. In doing so, we have theoretically identified strongly interacting plant chemicals and their biomolecular targets. These results should lead to further research to verify the efficacy of the phytochemical agents as well as delineate possible modifications of the active compounds to increase potency or selectivity.

Nigerian plants, but most of the bioactive components of those plants have not been characterized. However, the country's big and loosely-regulated traditional medicine industry continues to promote the efficacy of extracts and concoctions made from most of the plants. A number of Nigerian plants have been used traditionally in West Africa to treat protozoal infections and many of these have shown *in-vitro* antiprotozoal activity (Table S1).

Several *T. brucei* protein targets have been identified and experimentally validated [6]. In addition to validated targets, several potential targets have been predicted *in silico* [7]. For a recent review of phytochemical agents that show activities against parasitic protozoans and protozoan biochemical targets, see [8,9]. Some of the potential *T. brucei* drug targets that we considered in this work include adenosine kinase [10], pteridine reductase 1 [11], dihydrofolate reductase [12], trypanothione reductase [13], cathepsin B [14], heat shock protein 90 [15], as well as sterol 14α-demethylase (CYP51) [16], nucleoside hydrolase [17], triose phosphate isomerase [18], nucleoside 2-deoxyribosyltransferase [19], UDP-galactose 4′ epimerase [20] and ornithine decarboxylase [21]. In this computational study, we have evaluated the interaction of compounds that were isolated from some antitrypanosomal Nigerian medicinal plants (Table S1) against potential protein drug targets in *Trypanosoma brucei* for which X-ray crystal structures were available from the Protein Data Bank (PDB). We strove to address the questions of which phytochemical agents might be responsible for the observed antitrypanosomal activity and what are the likely targets of those phytochemicals. In doing so, we hope to identify particular classes of phytochemical agents that can be exploited for antiparasitic chemotherapy.

Methods

Protein-ligand docking studies were carried out based on the crystal structures of rhodesain (PDB 2p7u, [22] and PDB 2p86 [23]), *T. brucei* adenosine kinase, TbAK (PDB 2xtb and PDB 3otx [24]), *T. brucei* pteridine reductase 1, TbPTR1 (PDB 3jq7 [25]), *T. brucei* dihydrofolate reductase, TbDHFR (PDB 3rg9 and PDB 3qfx [26]), *T. brucei* trypanothione reductase, TbTR (PDB 2wow, [27]), *T. brucei* cathepsin B, TbCatB (PDB 3hhi [28]), *T. brucei* heat shock protein 90, TbHSP90 (PDB 3omu [29] and PDB 3opd [30]), *T.*

brucei sterol 14α-demethylase, TbCYP51 (PDB 3gw9 [16]), *T. brucei* nucleoside hydrolase, TbNH (PDB 3fz0 [31]), *T. brucei* triosephosphate isomerase, TbTIM (PDB 1iih, PDB 6tim [32], and PDB 4tim [33]), *T. brucei* nucleoside 2-deoxyribosyltransferase, TbNDRT (PDB 2a0k, PDB 2f64, and PDB 2f67 [19]), *T. brucei* UDP-galactose 4′-epimerase, TbUDPGE (PDB 1gy8 [20]), and *T. brucei* ornithine decarboxylase, TbODC (PDB 1f3t [34], PDB 1njj [35], and PDB 1qu4 [21]). All solvent molecules and the co-crystallized ligands were removed from the structures. Molecular docking calculations for all compounds with each of the proteins were undertaken using Molegro Virtual Docker v. 4.3 [36,37], with a sphere large enough to accommodate the cavity centered on the binding sites of each protein structure in order to allow each ligand to search. If a co-crystallized inhibitor or substrate was present in the structure, then that site was chosen as the binding site. If no co-crystallized ligand was present, then suitably sized cavities were used as potential binding sites. Standard protonation states of the proteins based on neutral pH were used in the docking studies. The protein was used as a rigid model structure; no relaxation of the protein was performed. Assignments of charges on each protein were based on standard templates as part of the Molegro Virtual Docker program; no other charges were set. Each ligand structure was built using Spartan '08 for Windows [38]. The structures were geometry optimized using the MMFF force field [39]. Flexible ligand models were used in the docking and subsequent optimization scheme. As a test of docking accuracy and for docking energy comparison, co-crystallized ligands were re-docked into the protein structures. Different orientations of the ligands were searched and ranked based on their energy scores. The RMSD threshold for multiple cluster poses was set at <1.00 Å. The docking algorithm was set at maximum iterations of 1500 with a simplex evolution population size of 50 and a minimum of 30 runs for each ligand. Each binding site of oligomeric structures was searched with each ligand. The lowest-energy (strongest-docking) poses for each ligand in each protein target are summarized in Tables S2–S20.

Results and Discussion

Acacia nilotica

Phytochemical studies of *Acacia nilotica* [40–45] have shown an abundance of polyphenolic compounds (Table S2), including hydrolyzable tannins, flavonoid gallates, and flavonoid glycosides. Although these polyphenolics are notorious for being promiscuous protein complexing agents and they do show relatively strong docking to all proteins investigated in this study, some selectivity can be seen. Thus, for example, 1,3-digalloylglucose showed docking selectivity for TbUDPGE, 3′,5-digalloylcatechin was selective for TbAK, and 3′,7-digalloylcatechin selectively docked with TbNH and was the strongest binding ligand for that protein (−44.2 kcal/mol). 5,7-Digalloylcatechin was the strongest binding ligand for TbPTR1 (−42.7 kcal/mol) and 4′,7-digalloylcatechin was the strongest binding ligand for TbODC (−41.4 kcal/mol). A number of these polyphenolic ligands showed strong docking interactions with TbAK, TbPTR1, TbCYP51, TbNH, and TbUDPGE, and interactions with these protein targets may be responsible for the antitrypanosomal activity of *A. nilotica* [46]. The docking study suggests that rhodesain, TbDHFR, TbTR, TbCatB, and TbHSP90 are not targets for *A. nilotica* phytochemicals.

Ageratum conyzoides

Ageratum conyzoides extracts have been dominated by flavonoids and chromanes (Table S3) [40,47–49]. 5,6-Dimethoxy-2-isopropylbenzofuran,6,7-dimethoxy-2-methyl-2-(2-methyl-1-propanone)-

3-chromene, 6-acetyl-2,2-dimethylchroman, and *O*-methylenece-calinol exhibited selectivity for TbTIM with docking energies comparable to the co-crystallized ligand, 3-phosphoglyceric acid (-21.6 kcal/mol). The flavonoid 3′,4′,5,5′,6,8-hexamethoxyfla-vone, on the other hand, showed selective docking to TbPTR1 and TbUDPGE. Nour and co-workers [49] have examined the antitrypanosomal activities of several methylated flavonoids and a chromene from *A. conyzoides*. The flavonoids all have similar antitrypanosomal activities with IC_{50} values ranging from 3.0 to 6.7 µg/mL. The chromene, *O*-methylencedalinol, on the other hand, was much less active ($IC_{50} = 78.4$ µg/mL). The docking energies for many of the protein targets was much more negative (stronger docking) for the flavonoids than for the chromene. Thus, for example, there is good correlation between $\log(IC_{50})$ and docking energies of the ligands with TbPTR1 or with TbUDPGE ($R^2 = 0.712$ and 0.751, respectively).

Annona senegalensis

Compounds isolated from *Annona senegalensis* include annonaceous acetogenins, diterpenoids, and sesquiterpenoids, and aporphine alkaloids (Table S4) [40,50–53]. The acetogenins (annogalene, annonacin, annonacin A, annosenegalin, and senegalene) are probably responsible for the antitrypanosomal activity of the plant

[54,55]. These compounds show a propensity for docking with TbAK, TbCYP51, and TbUDPGE. The acetogenins are very flexible with a great deal of conformational mobility. Nevertheless, docking with these protein targets is largely hydrophobic. Key interactions of the acetogenins with TbAK include Phe337, Gly298, Asn295, Asn67, and Gly296. Additionally, the acetogenin annogalene is one of the best binding ligands for TbDPGE (-42.9 kcal/mol).

Bridelia ferruginea

Bridelia ferruginea has been phytochemically characterized with polyphenolic and triterpenoid constituents (Table S5) [40,56]. The flavonoids delphinidin and ferrugin showed docking selectivity for TbPTR1. The tannin epigallocatechin(7→4′)gallocatechin showed notably strong docking with TbCYP51. Although they are relatively weak docking ligands, the triterpenoids friedelin and taraxerol docked selectively with TbUDPGE.

Carapa procera

Limonoids are characteristic phytochemicals of the Meliaceae, including *Carapa procera* (Table S6) [40,57], and numerous limonoids have exhibited antiprotozoal activities [58–62]. Six of the eleven *C. procera* limonoids showed notably strong docking with
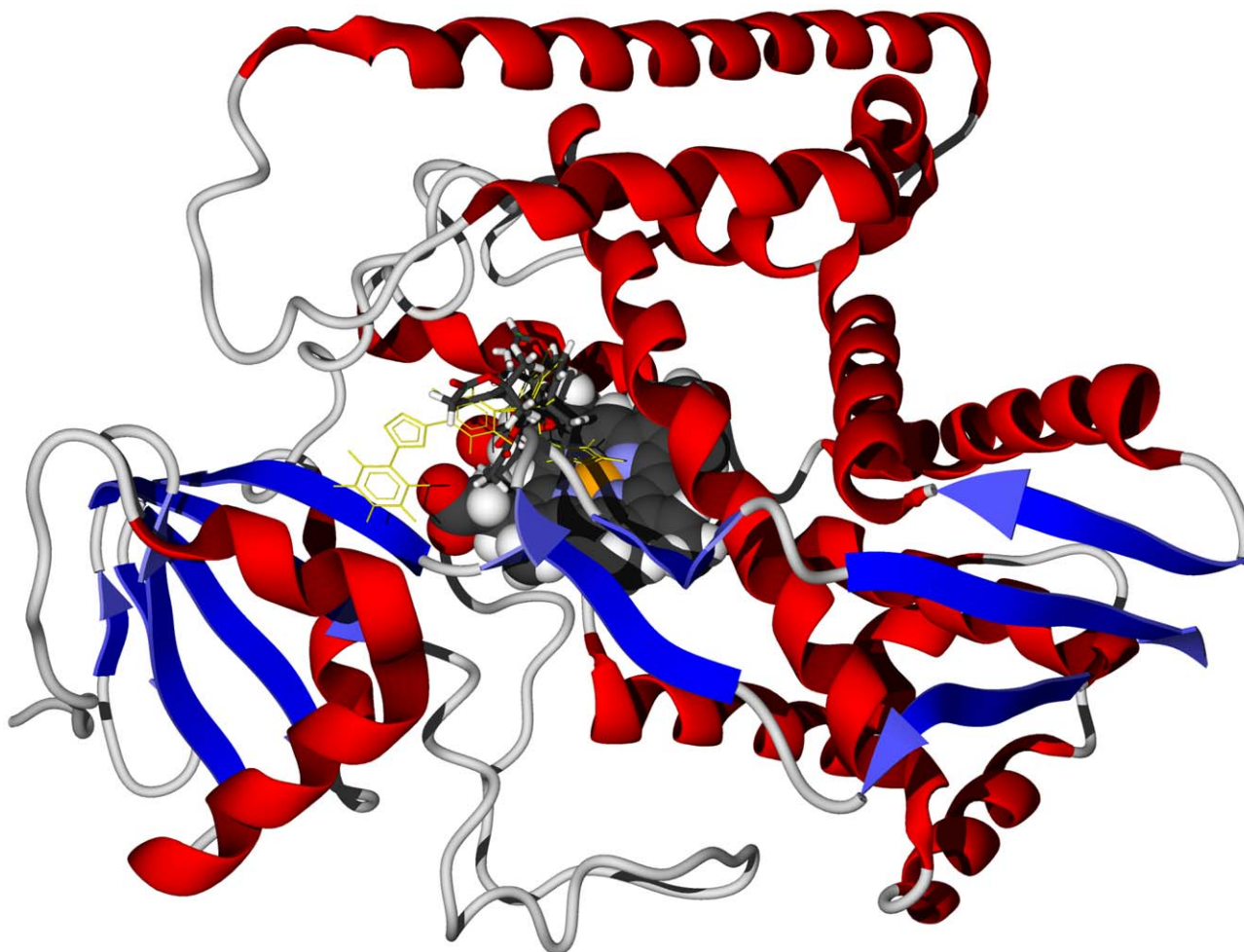
Figure 1. The crystal structure of *T. brucei* sterol 14α-demethylase, TbCYP51 (PDB 3gw9) [34]. The docked ligand is carapolide A (stick figure). The co-crystallized ligand is shown as a green wire figure and the heme cofactor is shown as a space-filling structure.
doi:10.1371/journal.pntd.0001727.g001
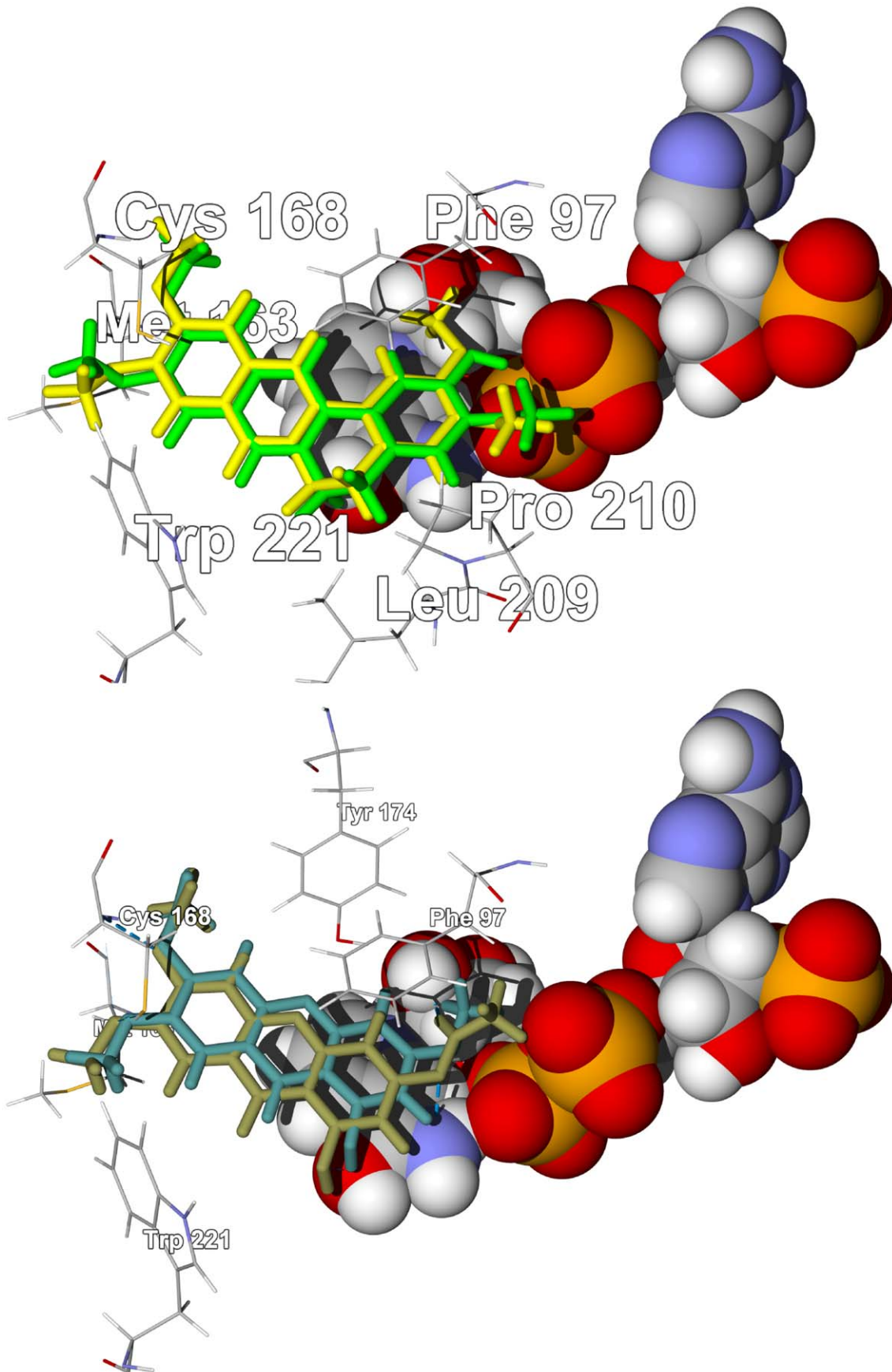
Figure 2. The crystal structure of *T. brucei* pteridine reductase 1, TbPTR1 (PDB 3jq7) [43]. Top: Lowest-energy docking poses of pseudocolumbamine (green stick figure) and pseudopalmatine (yellow stick figure) in the crystal structure. The NADP$^+$ cofactor is shown as a space-filling structure. Bottom: Lowest-energy docking poses of laxanthone II (brown stick figure) and laxanthone III (dark green stick figure) in the same crystal structure.
doi:10.1371/journal.pntd.0001727.g002

TbCYP51 (docking energies <−26 kcal/mol). A similar trend was noted for docking of *Khaya* limonoids (see below). Carapolides A, B, and C showed particularly strong docking with docking energies of −31.8, −29.3, and −28.5 kcal/mol, respectively; comparable to the docking energy of the co-crystallized ligand, *N*-[(1*R*)-1-(2,4-dichlorophenyl)-2-(1*H*-imidazol-1-yl)ethyl]-4-(5-phenyl-1,3,4-oxa-diazol-2-yl)benzamide [16] (−28.6 kcal/mol), for this protein. The limonoids all dock with TbCYP51 near the heme cofactor (Fig. 1). In addition, preferential docking of individual limonoids with other protein targets include: mexicanolide with TbAK, 3β-isobutyroloxy-1-oxomeliac-8(30)-enate with TbPTR1, and evodulone with TbCatB. We conclude, therefore, that *T. brucei* sterol 14α-demethylase, TbCYP51, is a protein target of *C. procera* limonoids.

Enantia chlorantha

Enantia chlorantha is dominated by aporphine and berberine alkaloids (Table S7) [40,63,64]. *E. chlorantha* aporphine alkaloids seem to show a propensity for docking with TbPTR1 or with TbUDPGE while the berberine alkaloids showed selectivity for TbPTR1. Both pseudocolumbamine and pseudopalmatine docked with TbPTR1 with docking energies (−27.5 kcal/mol) comparable to the co-crystallized ligand, 6-phenylpteridine-2,4,7-triamine [25] (−27.6 kcal/mol). These planar alkaloids dock into the active site by way of hydrophobic interactions with the NADP$^+$ cofactor and a hydrophobic pocket formed by Phe97, Met163, Cys168, Pro210, Trp221, and Leu209 (Fig. 2). Liriodenine and columbamine docked selectively to TbTIM with docking energies lower (−24.0 and −24.7 kcal/mol) than the co-crystallized ligand, 3-
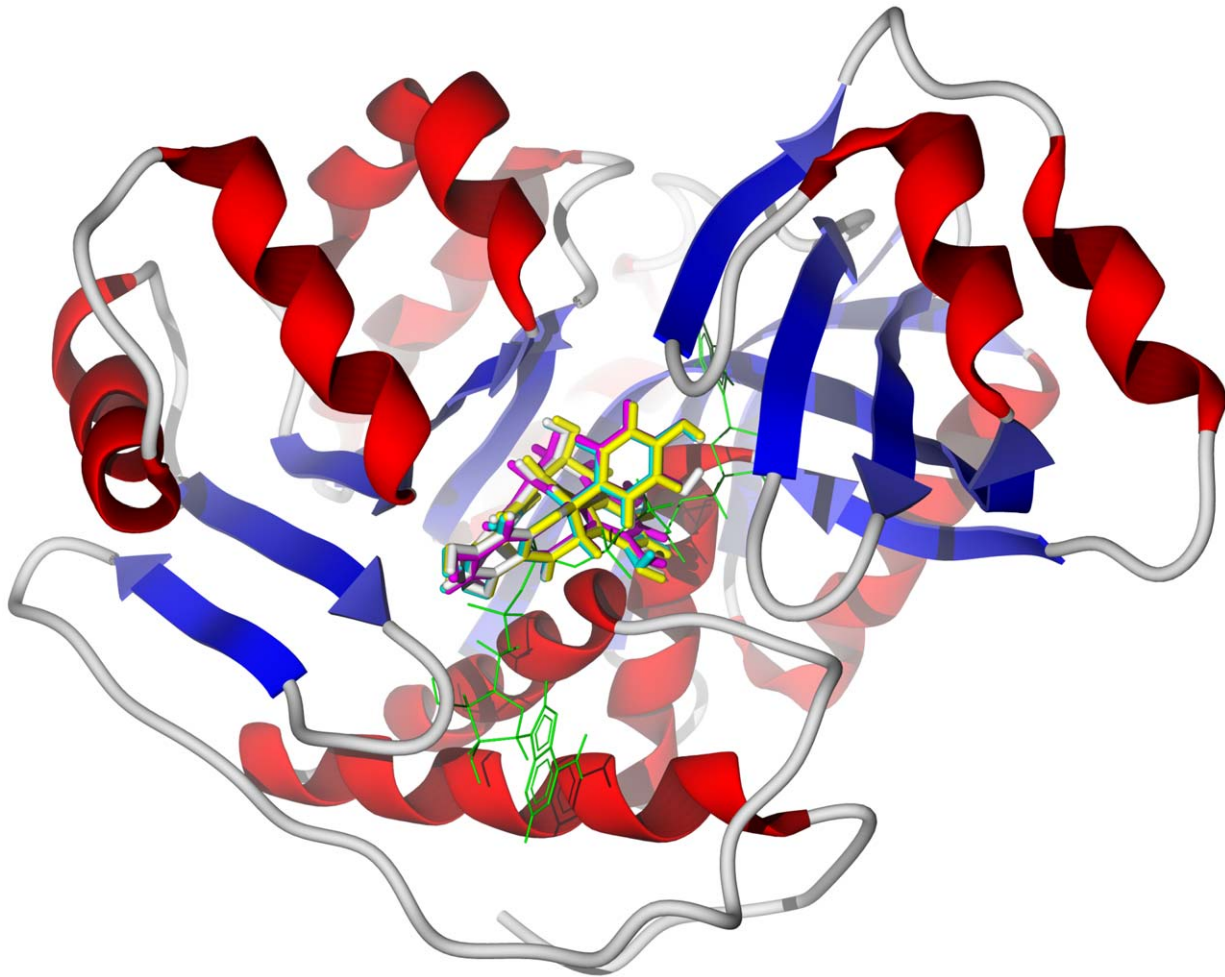
Figure 3. The crystal structure of *T. brucei* adenosine kinase, TbAK (PDB 3otx) [42]. The docked poses are the biflavonoids GB1 (turquoise), GB1a (magenta), GB2 (yellow), and garciniflavanone (white). The co-crystallized ligand, *bis*(adenosine)-5′-pentaphosphate, is shown as a green wire figure.
doi:10.1371/journal.pntd.0001727.g003
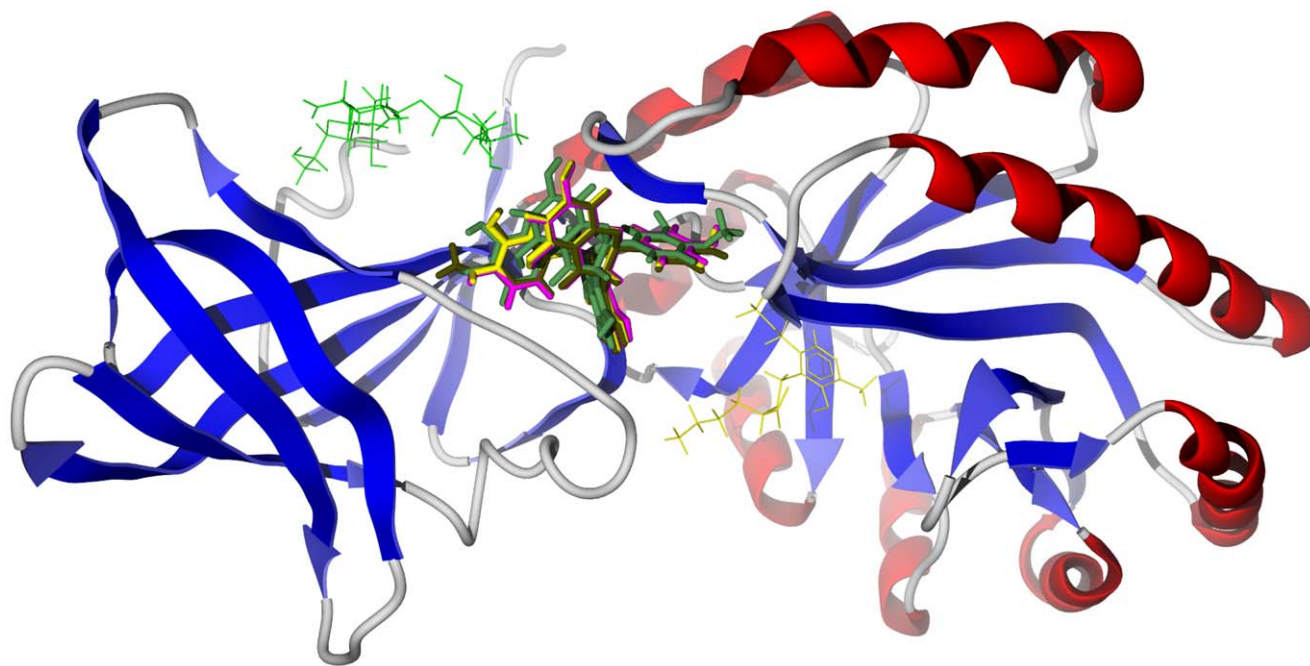
Figure 4. The crystal structure of *T. brucei* ornithine decarboxylase, TbODC (PDB 1njj) [53]**.** The docked poses are the biflavonoids GB1a (magenta), GB2 (yellow), GB3 (green) and kolaflavanone (brown). The co-crystallized ligands are geneticin (green wire figure) and pyridoxylphosphate/D-ornithine (yellow wire figure).
doi:10.1371/journal.pntd.0001727.g004

phosphoglyceric acid [32] (−21.6 kcal/mol). These nearly planar alkaloids are known also to be DNA intercalators and topoisomerase inhibitors [65].

Garcinia kola

Polyphenolic compounds, flavonoids, biflavonoids, etc., have been isolated and identified from *Garcinia kola* (Table S8) [40,66]. *G. kola* biflavonoids docked favorably with TbAK and TbODC. The biflavonoids do not dock at the adenosine binding sites of TbAK, but rather in a pocket between the two sites bounded by residues Asn222, Gly298, Ala297, Thr264, Asp266, Glu225, Arg132, and Asn195 (see Fig. 3). Likewise, biflavonoid docking with TbODC does not occur at the ornithine/putrescine binding site or the geneticin binding site, but rather in a pocket bounded by Asp243, Asp385, Val335, Asp332, Ala334, Ala244, and Arg277 (Fig. 4). This would suggest that if *G. kola* biflavonoids inhibit either TbAK or TbODC, they act as allosteric inhibitors of these proteins. The two tocotrienols garcinal and garcinoic acid, on the other hand, docked more favorably with TbUDPGE. Key interactions of the tocotrienols with the protein are hydrogen-bonding of the phenolic –OH of the ligands with Pro253 and Phe255, hydrogen-bonding of the carbonyl group of the ligand side chains with Arg268, hydrogen-bonding of the pyran ring oxygen atom with Arg235, face-to-face $\pi - \pi$ interactions of the ligand aromatic rings with Phe255, and hydrophobic interactions of the tocotrienol ligands with Leu222, His221 and the NAD cofactor (Fig. 5 top). The prenylated benzophenone kolanone docked very strongly with TbNH (docking energy = −37.1 kcal/mol) in the nucleoside binding site (Fig. 6), a hydrophobic pocket bounded by Trp80, Phe178, Asn171, Trp205, and Val277, with additional hydrogen-bonding with Asn171.

Khaya ivorensis and Khaya senegalensis

The phytochemical compositions of *Khaya ivorensis* [67] and *K. senegalensis* [58,68–72], like other members of the Meliaceae, are characterized by limonoids [40]. Many of the *Khaya* limonoids showed markedly strong docking to TbAK as well as TbCYP51 (see Table S9). Of particular note, 3-*O*-acetylkhayalactone strongly docked with TbAK, TbDHFR, and TbUDPGE (−31.6, −32.2, and −34.2 kcal/mol, respectively). This ligand docked in the same site in TbAK as the *Garcinia* biflavonoids (above), but in a different position in TbUDPGE (Fig. 5 bottom). Important hydrogen-bonding interactions of 3-*O*-acetylkhayalactone with TbUDPGE are with residues Glu214, Ser219, Leu102, Thr220, and His221. 3-*O*-Acetylkhayalactone docked in the active site of TbDHFR in the same general location as the co-crystallized ligand (Fig. 7). In addition, the docking energy of 3-*O*-acetylkhayalactone (−32.2 kcal/mol) was lower than either of the co-crystallized ligands, 5-(4-chlorophenyl)-6-ethylpyrimidine-2,4-diamine (pyrimethamine) and 6,6-dimethyl-1-[3-(2,4,5-trichlorophenoxy)propoxy]-1,6-dihydro-1,3,5-triazine-2,4-diamine [26] (−22.7 and −30.1 kcal/mol, respectively). In general, the *Khaya* limonoids showed weak or no docking with TbNH, TbTIM, or TbNDRT.

Lawsonia inermis

The sterols and triterpenoids [40] from *Lawsonia inermis* showed preferential docking to TbCYP51 (*T. brucei* sterol 14α-demethylase) (Table S10). This is perhaps not surprising since the normal substrates for this enzyme are sterols. The laxanthones from *L. inermis* showed preferential docking to TbPTR1 with docking energies comparable to the co-crystallized ligand. In addition, they docked in the same positions and orientations as pseudocolumbamine and pseudopalmatine from *Enantia chlorantha* (see above and Fig. 2).
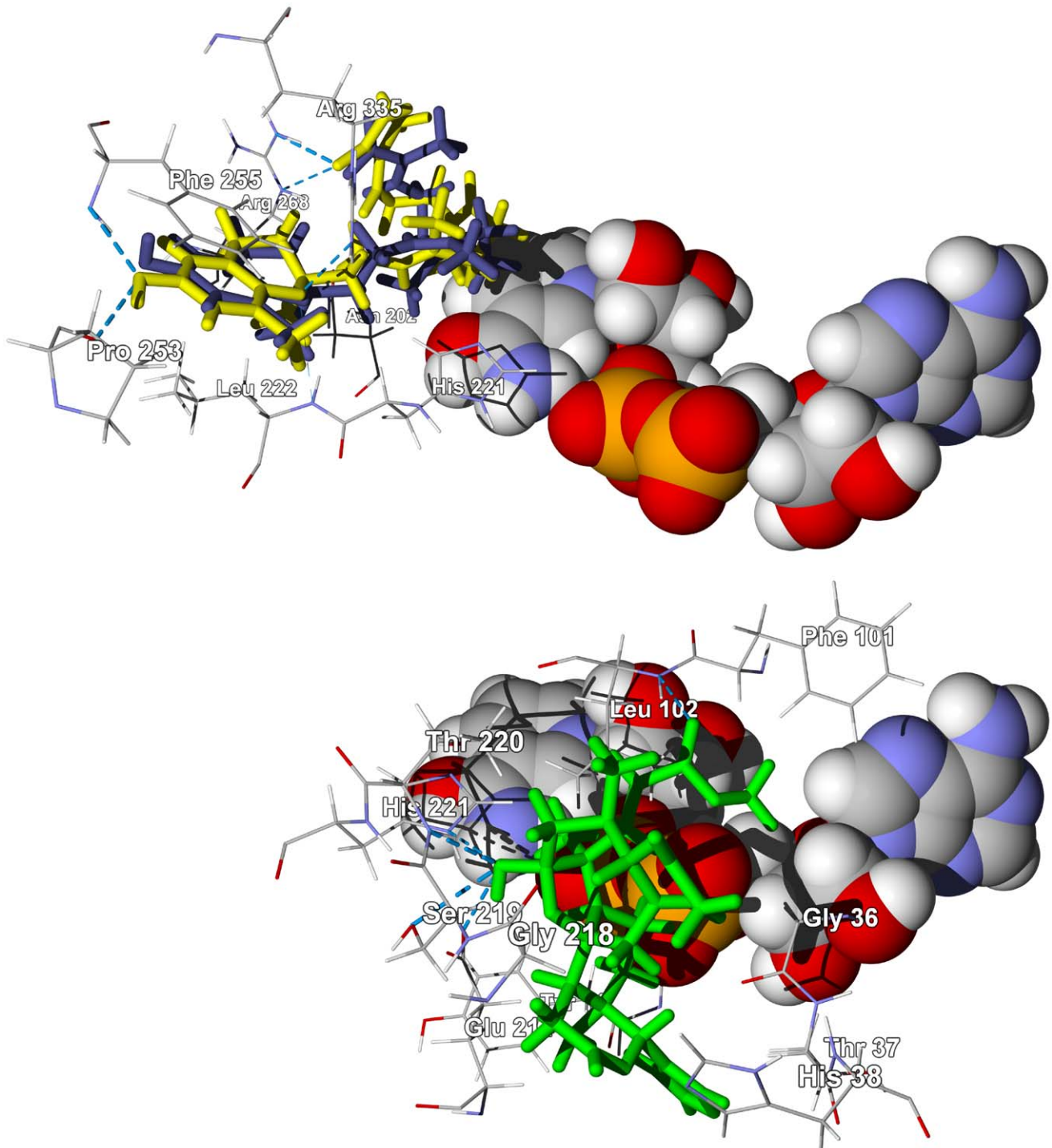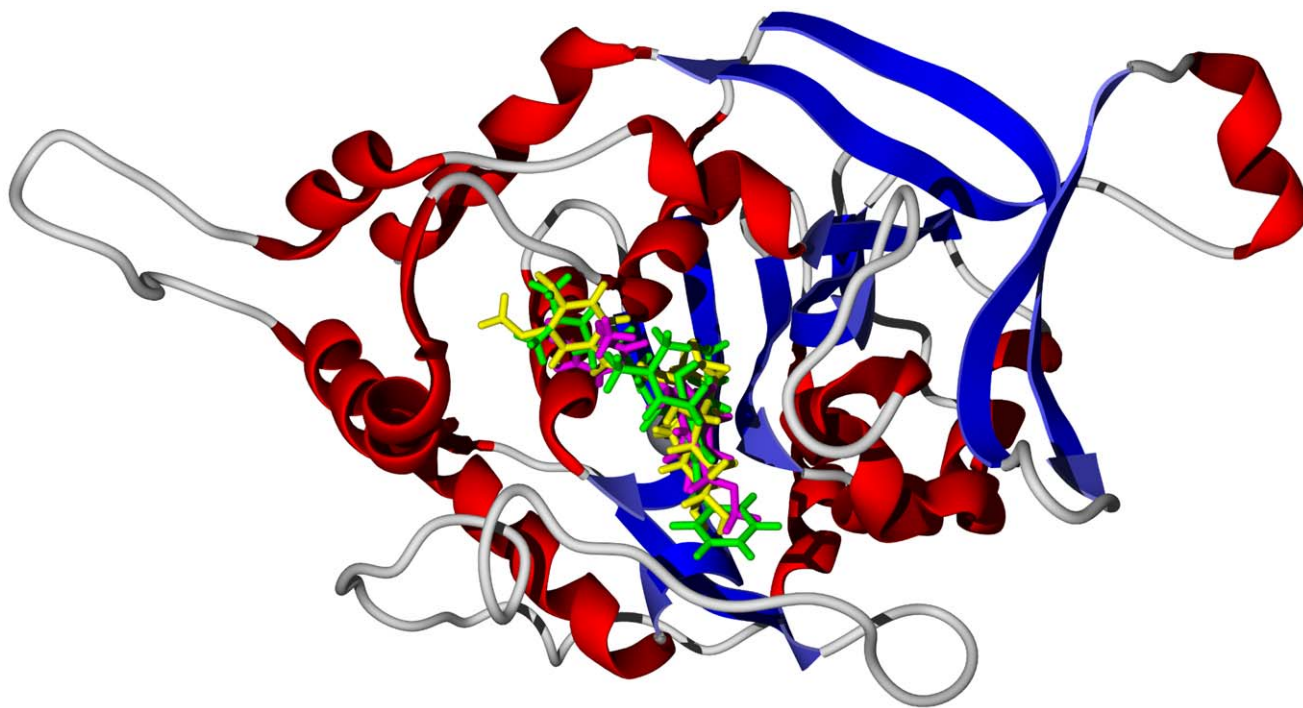
Figure 5. The crystal structure of *T. brucei* **UDP-galactose 4′-epimerase, TbUDPGE (PDB 1gy8)** [37]. Top: Lowest-energy docked poses of garcinal (purple stick figure) and garcinoic acid (yellow stick figure) showing key hydrogen-bonding and hydrophobic interactions. The NAD cofactor is shown as a space-filling structure; hydrogen bonds are depicted as blue dashed lines. Bottom: Lowest-energy docked pose of 3-*O*-acetylkhayalactone (green stick figure) in the same crystal structure.
doi:10.1371/journal.pntd.0001727.g005

Morinda lucida

Anthraquinones dominate the phytochemistry of *Morinda lucida* [40,73,74], along with triterpenoid acids [75] (see Table S11). Anthraquinones, as a class, demonstrated significant docking affinity for TbPRT1 and TbTIM (Fig. 8). Anthraquinones are also known to be DNA intercalators and topoisomerase inhibitors [76]. The triterpenoid acids oleanolic acid and ursolic acid showed notable docking energies with TbCYP51 (see above). The phenylpropanoid

Figure 6. The X-ray crystal structure of *T. brucei* nucleoside hydrolase, Tb NH (PDB 3fz0) [49]. The lowest energy docking poses of kolanone (green), oruwacin (magenta), and dehydroepoxymethoxygaertneroside (yellow) are shown in the active site.
doi:10.1371/journal.pntd.0001727.g006

oruwacin docked very strongly to TbPTR1 (docking energy = −32.4 kcal/mol) and TbNH (docking energy = −31.6 kcal/mol, Fig. 6).

Morinda morindoides

The phytochemistry of *Morinda morindoides* [40] is dominated by flavonoid glycosides [77] and phenylpropanoid-conjugated iridoid glycosides [78] (Table S12). Of these, epoxygaertneroside and morindaoside were selectively strongly binding ligands for TbAK, and morindaoside also docked strongly to TbPTR1. A number of gaertneroside derivatives showed docking selectivity for TbDHFR (see Table S12), while dehydroepoxymethoxygaertneroside docked very strongly with TbNH, occupying the nucleoside binding site (Fig. 6) with the same hydrophobic interactions as kolanone and oruwacin (above). It is unlikely that these glycosides will remain intact *in vivo*, and hydrolysis may be necessary for absorption and general bioavailability [79]. Of the flavonoid aglycones from *M. morindoides*, apigenin, chrysoeriol, kaempferol, quercetin, and ombuin selectively docked with TbPTR1.

Nauclea latifolia

Phytochemical investigations of *Nauclea latifolia* have revealed numerous indole alkaloids [40,80,81] (Table S13). The alkaloid glycosides 10-hydroxystrictosamide, cadambine, dihydrocadambine, and tetrahydrodesoxycordifoline showed notably strong docking to TbUDPGE, whereas non-glycosylated alkaloids showed preferential docking with TbPTR1and/or TbAK. 10-Hydroxyangustine, angustine, naucleamide B, and naucletine, in particular, docked more strongly with TbPTR1 than the co-crystallized ligand, 6-phenylpteridine-2,4,7-triamine [25] (docking energy = −27.6 kcal/mol).

Newbouldia laevis

T. brucei triosephosphate isomerase, TbTIM, is the likely protein target for the phytochemical agents of *Newbouldia laevis*. Both furanonaphthoquinones [82,83] and pyrazole alkaloids [84,85] from this plant showed remarkable selective affinity for this protein (Table S14). The monomeric furanonaphthoquinone ligands all occupy the same site with hydrogen bonding of the furan oxygen and C(9) carbonyl oxygen to Lys313; C(4) carbonyl oxygen with Ser513 and Val514; a van der Waals surface provided by Val533, Gly534, Gly535; and a hydrophobic pocket to accommodate the isopropenyl moiety provided by Ile472, Gly512, and Leu532 (see Fig. 9). Similarly, the pyrazole alkaloid 4′-hydroxywithasomnine has key hydrogen-bonding interactions between the pyrazole ring nitrogens and Ser513 and Val514. The aromatic ring lies in the hydrophobic pocket made up of Ile472 and Leu532, and there is an additional hydrogen-bonding interaction between the phenolic –OH group and His395 (Fig. 9).

Physalis angulata

Withanolide triterpenoids, abundant components of *Physalis angulata* [40,86–88], generally showed preferential docking to *T. brucei* sterol 14α-demethylase, TbCYP51 (Table S15). This is consistent with the docking of *L. inermis* triterpenoids and steroids, *C. procera* and *Khaya* limonoids (see above). Five of the withanolides, 14-hydroxyixocarpanolide, physagulin J, physagulin L, withangulatin H, and withangulatin I, docked more strongly to TbCYP51 than the co-crystallized ligand [16]. Three withanolides, physagulin A, physagulin L′, and withangulatin A, docked more strongly into TbODC than the co-crystallized
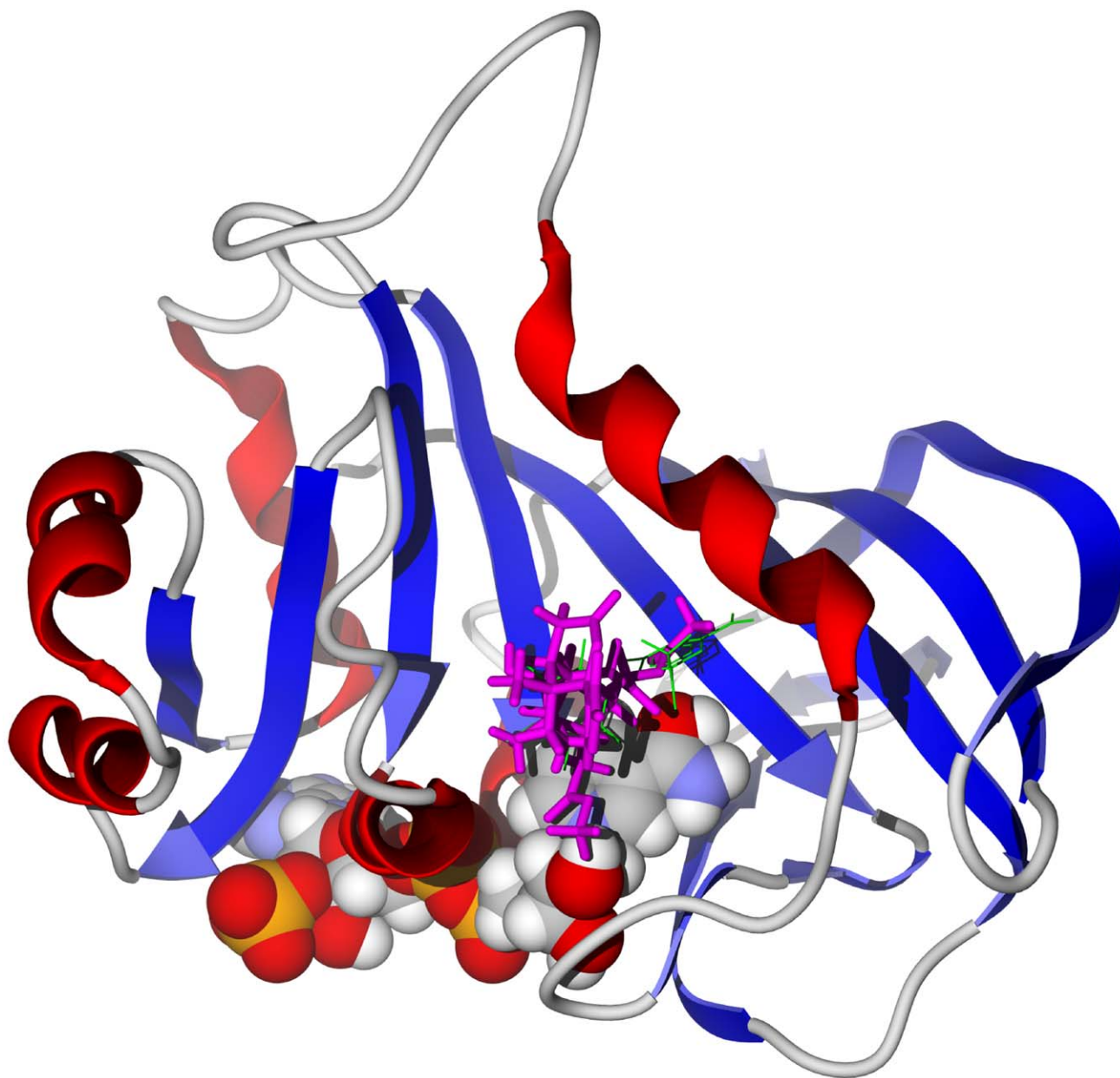
Figure 7. The crystal structure of *T. brucei* dihydrofolate reductase, TbDHFR (PDB 3qfx) [**44**]. The docked structure is 3-*O*-acetylkhayalactone (magenta). The co-crystallized ligand, pyrimethamine, is shown as a green wire figure and the NADPH cofactor as a space-filling structure.
doi:10.1371/journal.pntd.0001727.g007

ligand (pyridoxal 5′-phosphate) for that protein [34]. The pyrrolidine alkaloid, phygrine, docked with TbTIM preferentially.

Picralima nitida

Picralima nitida glycosylated coumestans [89] showed strong binding to most of the protein targets, except for TbNDRT (Table S16). They are, for example, along with *Acacia nilotica* flavonoid gallates, the only ligands that dock to rhodesain with docking energies comparable to the co-crystallized ligand. Of the ligands

examined in this work, coumestan **2** is the strongest-binding ligand for TbAK (−44.1 kcal/mol) and TbUDPGE (−43.7 kcal/mol). The corresponding aglycones, **4**, **5**, and **6**, however, were selective for TbPTR1 as well as TbUDPGE.

Prosopis africana

The phytochemistry of *Prosopis africana* is characterized by piperidine alkaloids (Table S17) [40,90]. These ligands exhibited similar docking energies with all protein targets, owing presumably to the small, flexible nature of the compounds. They did, however, show slightly better affinity for TbAK.
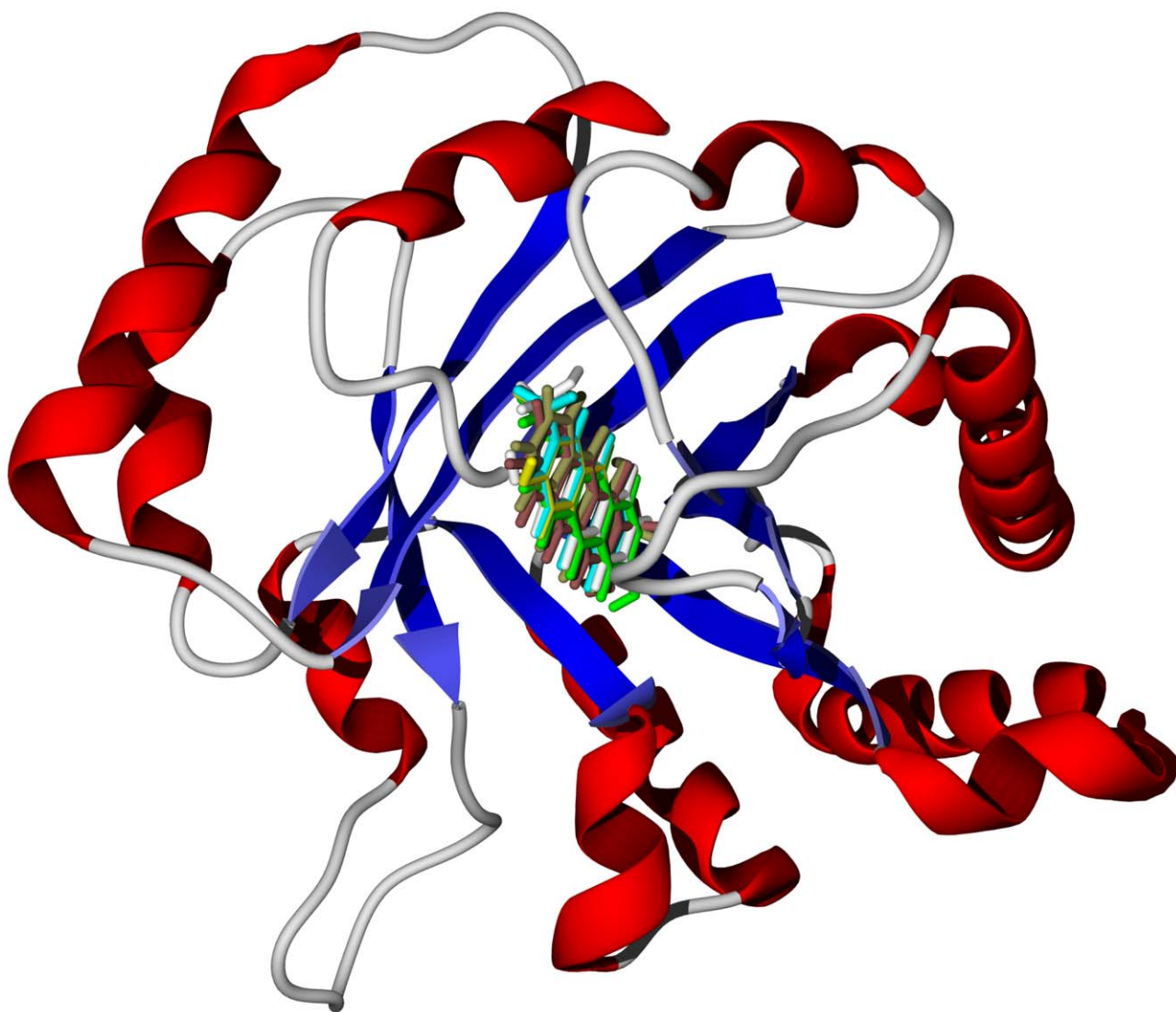
Figure 8. The crystal structure of *T. brucei* triosephosphate isomerase, TbTIM (PDB 1iih) [**50**]**.** The docked structures are the lowest-energy docking poses of the strongly docking *M. lucida* anthraquinones (2-formyl-3-hydroxyanthaquinone, 2-formylanthraquinone, 2-hydroxy-3-hydroxymethyl-anthraquinone, nordamnacanthal, rubiadin, and soranjidiol) in the active site of the protein.
doi:10.1371/journal.pntd.0001727.g008

Rauwolfia vomitoria

Phytochemical investigations of *Rauwolfia vomitoria* have revealed this plant to be replete with indole alkaloids (Table S18) [40,91,92]. The structural diversity of these indole alkaloids seems to defy targeting any one particular protein. There are some notable docking results, however. 3-Epirescinnamine docked with TbPRT1 and with TbODC more strongly than the co-crystallized ligands, 6-phenylpteridine-2,4,7-triamine [25] and putrescine [34], respectively. Isoreserpiline, raumitorine, and rauvanine also docked strongly to TbPTR1. Ajmalimine, isoreserpiline, rauvo-mitine, and serpenticine had remarkable docking energies with TbNH. The trimethoxybenzoyl and trimethoxycinnamyl esters, renoxydine, rescidine, rescinnamine, reserpine, along with methyl 3,4-dimethoxybenzoylreserpate, were all excellent ligands for TbUDPGE, with docking energies comparable to uridine-5′-diphosphate, the co-crystallized ligand [20]. Of these, renoxydine, rescidine, and reserpine, along with neonorreserpine, docked strongly to TbCYP51.

Securidaca longipedunculata

Cinnamate esters from *Securidaca longipedunculata* [40] showed selective docking to TbTIM while *S. longipedunculata* xanthones [40,93] had a docking preference for TbPTR1. Both of these protein targets have relatively small binding sites, which are more suitable for the small ligands (Fig. 10). The xanthones also docked relatively strongly with TbUDPGE. The *S. longipedunculata* indole alkaloids dehydroelymoclavine and alkaloid A [94] docked strongly to TbPTR1 and TbAK, respectively, as well as with TbUDPGE (see Table S19).

### Strychnos spinosa

Phytochemicals isolated from *Strychnos spinosa* include secoir-idoids [95], indole, pyridine, and naphthyridine alkaloids [40], sterols and triterpenoids [96] (Table S20). Relatively small pyridine and naphthyridine alkaloids from *Strychnos spinosa* showed preferential docking to TbPTR1 and/or TbTIM. The indole alkaloids akagerine, 10-hydroxyakagerine, and kribine also docked
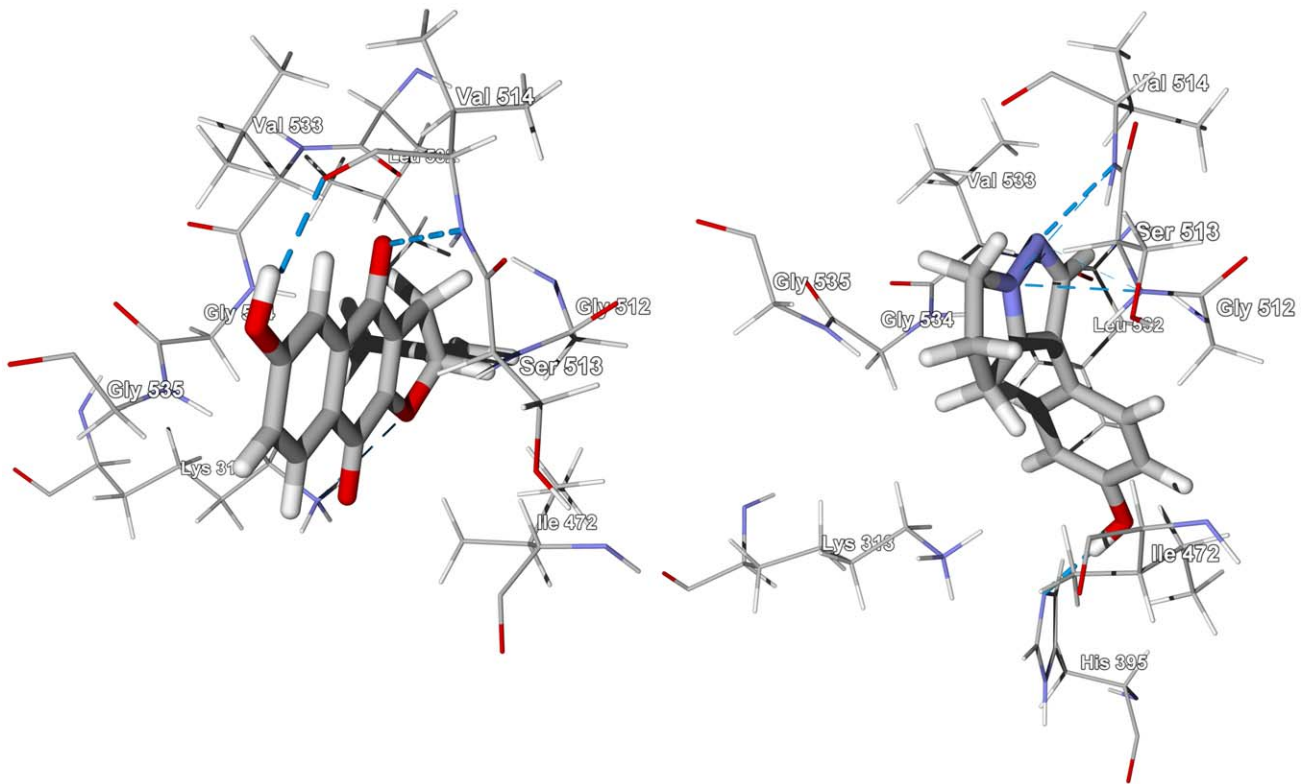
Figure 9. The crystal structure of *T. brucei* **triosephosphate isomerase, TbTIM (PDB 1iih)** [50]**.** The lowest-energy docking poses of 6-hydroxydehydroiso-α-lapachone (left) and 4′-hydroxywithasomnine (right) in the active site are shown. Hydrogen-bonding interactions are indicated by blue dashed lines.
doi:10.1371/journal.pntd.0001727.g009

preferentially to TbPTR1, while iridoid glucosides preferred TbUDPGE. Both sterols and triterpenoids from *S. spinosa* selectively docked with TbCYP51, similar to what was observed with *L. inermis* sterols and triterpenoids (see above), but these

compounds also showed notably strong docking with TbODC. Interestingly, a comparison of docking energies of triterpenoid and steroid ligands with their antitrypanosomal activities [96] shows no correlation, even comparing TbCYP51 docking or TbODC
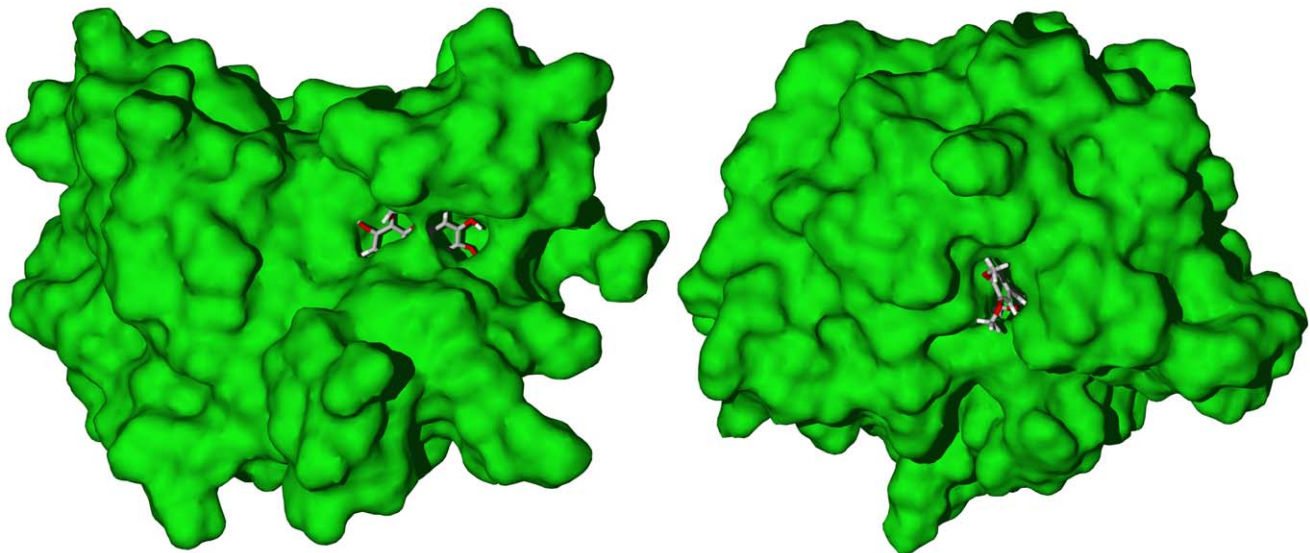
Figure 10. The crystal structure of *T. brucei* **pteridine reductase 1 (TbPTR1, PDB 3jq7** [43]**).** Left: Lowest-energy docked pose of 1,3,6,8-tetrahydro-2,5-dimethoxyxanthone. Right: Lowest-energy docked pose of (*E*)-ethyl 4-methoxycinnamate with *T. brucei* triosephosphate isomerase (TbTIM, PDB 1iih [50]).
doi:10.1371/journal.pntd.0001727.g010
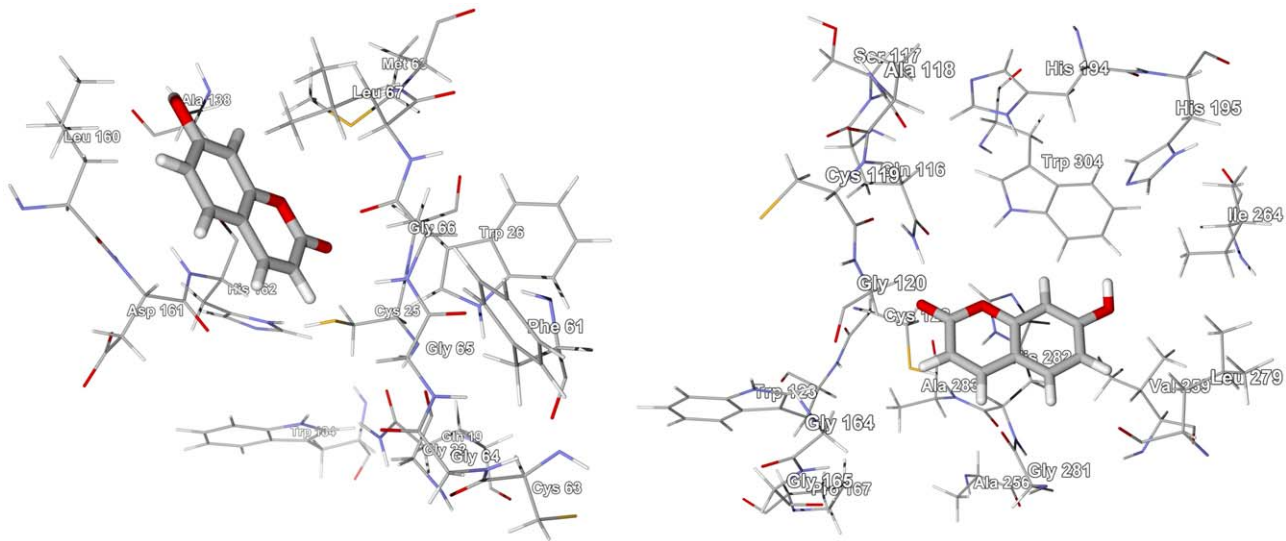
Figure 11. Docking poses of umbelliferone. Left: In the active sites of rhodesain (PDB 2p7u [40]). Right: In the active site of TbCatB (PDB 3hhi [46]).
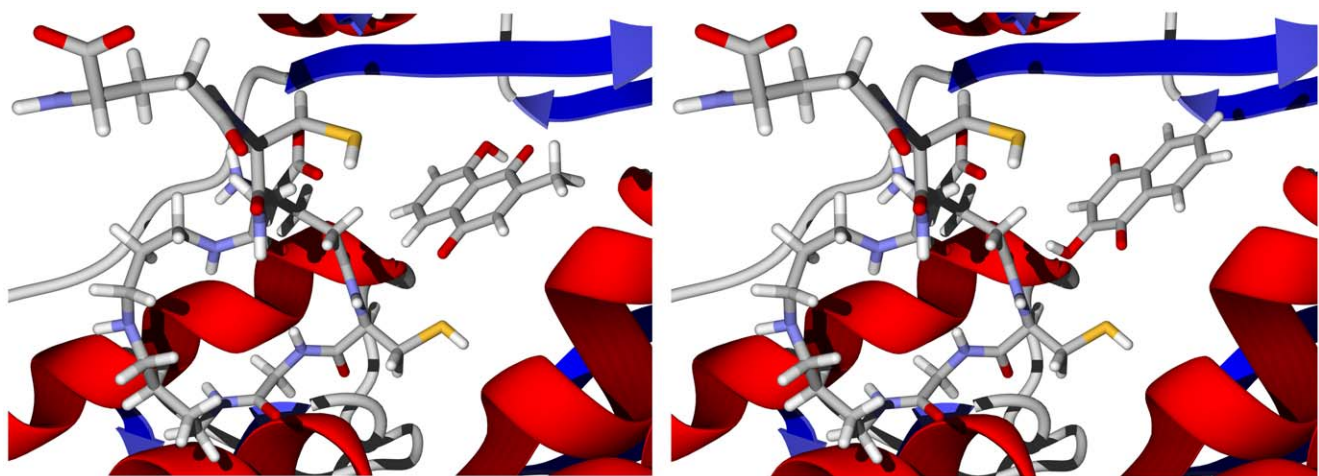doi:10.1371/journal.pntd.0001727.g011

docking. Plots of $\log(IC_{50})$ vs. docking energies gives R^2 values of 0.043 and 0.007 for TbCYP51 and TbODC, respectively. It may be that inhibition of some other protein target [8,9] is the biochemical mechanism of activity for these compounds.

In terms of natural products drug discovery, it is useful to examine whether different phytochemical classes show selectivity for particular protein targets. Simple flavonoid ligands showed docking preferences for TbPTR1 and TbUDPGE. Flavonoid gallates, on the other hand, were shown to be promiscuous docking ligands to all protein targets, but were particularly strongly docking with TbAK, TbPRT1, TbCYP51, and TbNH. Likewise, flavonoid glycosides tended to be promiscuous docking agents, but with preference for TbAK, TbPRT1, and TbNH. Oligomeric flavonoids (tannin-like polyphenolics) showed strong docking to TbAK. The diversity of flavonoid structures has led to diverse biological activities, including antiprotozoal activity, but the modes of antiprotozoal activity have not been well elucidated [97].

As previously noted (see above), triterpenoid ligands were largely selective for TbCYP51. Withanolide triterpenoids also showed a docking preference for TbCYP51, while limonoids preferentially docked with TbAK as well as TbCYP51. Not surprisingly, sterols showed a propensity to dock with TbCYP51, but also docked strongly with TbUDPGE.

All of the anthraquinone ligands examined in this docking study, docked with strong binding energies to TbPRT1. Likewise, xanthone ligands exhibited docking selectivity for TbPTR1. Naphthoquinones, on the other hand, docked preferentially with TbTIM. Most chromene ligands also showed notable docking energies to TbTIM. The phenylpropanoids examined showed preferences for TbTIM as well as TbUDPGE, while glycoside derivatives of phenylpropanoids showed selectivity for TbDHFR.

Berberine alkaloids docked preferentially to TbPTR1 while aporphine alkaloids showed some selectivity for TbPTR1 and TbUDPGE. Piperidine alkaloids were also selective for

Figure 12. The crystal structure of *T. brucei* **trypanothione reductase (TbTR, 2wow [45]).** The docked poses are isoplumbagin (left) and lawsone (right) in the proximity of trypanothione.
doi:10.1371/journal.pntd.0001727.g012
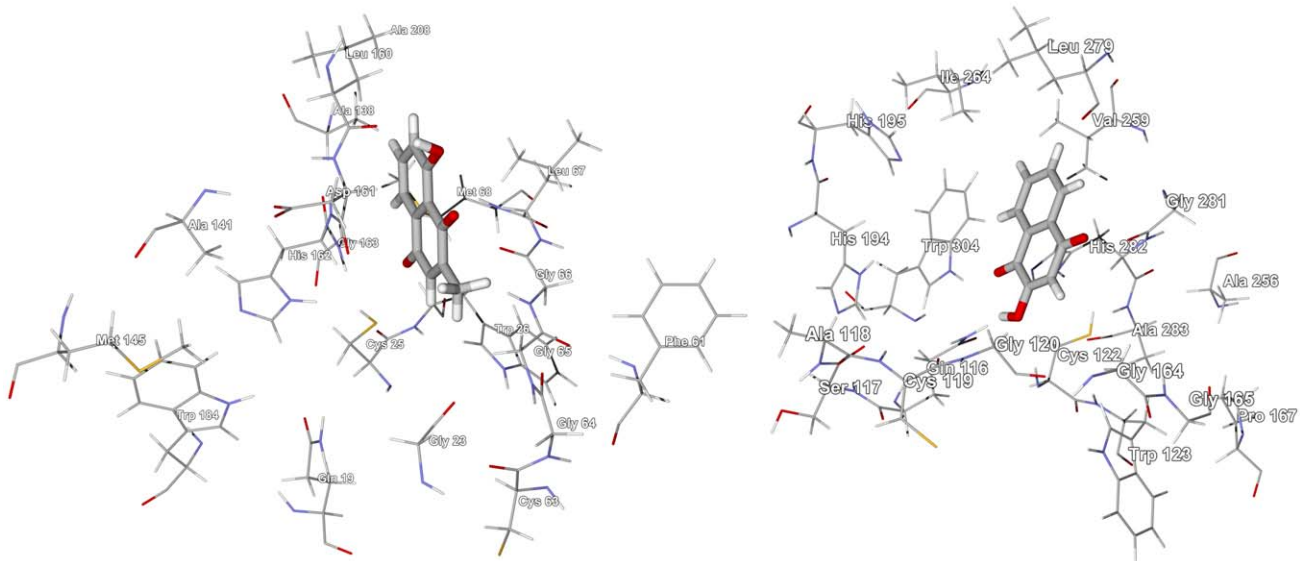
Figure 13. Left: Isoplumbagin in the active site of rhodesain (PDB 2p86 [41]). The S···C(3) = 3.18 Å. Right: Lowest-energy docked pose of lawsone in the active site of *T. brucei* cathepsin B (TbCatB, PDB 3hhi [46]; S···C(2) = 3.73 Å).
doi:10.1371/journal.pntd.0001727.g013

TbUDPGE. Pyrazole and pyridine alkaloids, on the other hand, preferred docking to TbTIM. A total of 93 indole alkaloids were examined in this docking study and many of them showed notable docking energies with TbUDPGE and some with TbAK and TbPTR1. Glycoside derivatives of alkaloids also preferentially docked with TbUDPGE.

Overall, the protein objects most targeted by the phytochemical ligands in this study were TbUDPGE, targeted by many alkaloids; TbPTR1, preferred by planar-like ligands; TbCYP51, which docked terpenoid ligands well; and TbAK, which docked many

different classes of phytochemicals. Those proteins least preferred in terms of docking energies were rhodesain, TbCatB, and TbNDRT.

Rhodesain and TbCatB are both cysteine proteases with relatively small binding sites. It may be that the docking energies reflect the fact that only relatively small ligands, with inherently small docking energies, can fit well into the binding sites of these two proteins. The docking energies do not, however, reflect the potential for covalent bonding to the active sites of these proteins. It is useful, therefore, to examine small electrophilic ligands for
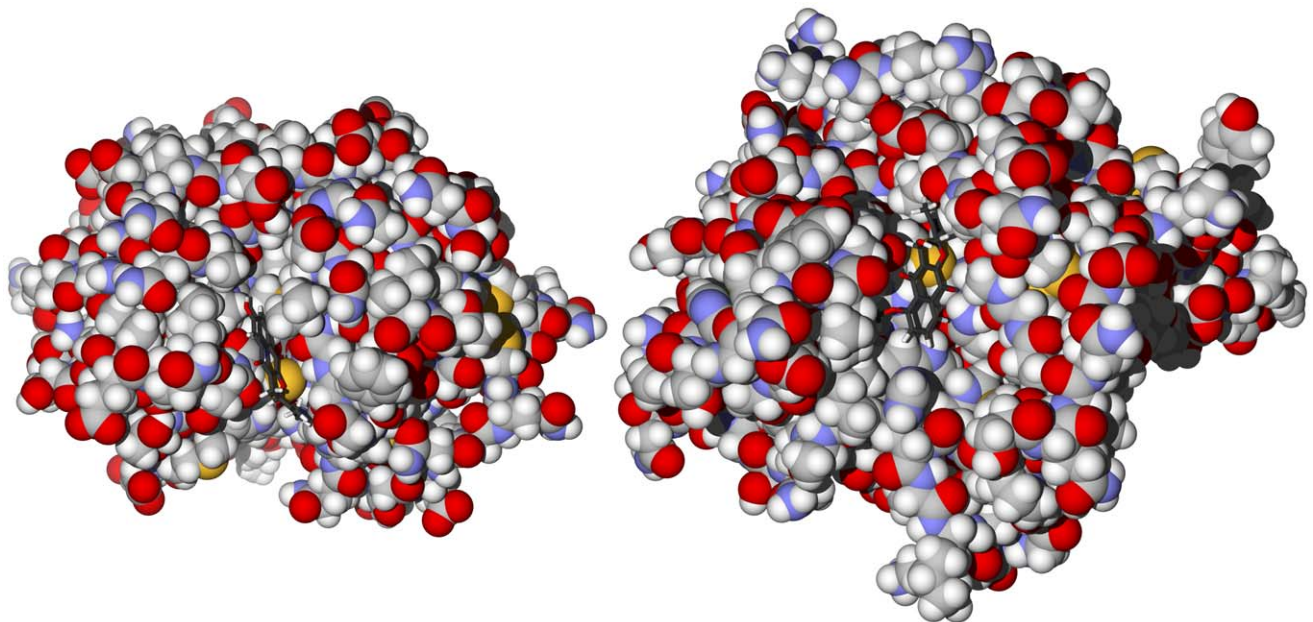
Figure 14. Lowest-energy docked poses of 6-hydroxydehydroiso-α-lapachone. Left: With rhodesain (PDB 2p86 [41]). Right: With TbCatB (PDB 3hhi [46]). Note the proximity and orientation of the quinone moiety with the cysteine sulfur atoms in the active sites.
doi:10.1371/journal.pntd.0001727.g014

energetically favorable docking orientations that would allow for reaction of nucleophilic amino acid side chains to the electrophilic sites of the ligands.

Although umbelliferone does not dock with particularly strong energies to rhodesain or TbCatB, it does dock in poses such that the nucleophilic Cys25 of rhodesain or Cys122 of TbCatB are poised to undergo conjugate addition to the pyrone ring (Fig. 11). The S atom of Cys25 is 3.16 Å from C(4) of docked umbelliferone in rhodesain, while in TbCatB, Cys122 is 3.65 Å from C(4) of umbelliferone. Coumarins have been shown to be trypanocidal agents [98] and it has been suggested that umbelliferone undergoes conjugate addition with available cysteine thiol groups [99].

Many naphthoquinones have been shown to be antitrypanosomal [100], and are suspected to interfere with redox thiol metabolism by inhibition of TbTR [101,102]. There are docking poses, albeit not the lowest-energy poses, of isoplumbagin (docking pose energy = −9.9 kcal/mol) and lawsone (docking pose energy = −8.6 kcal/mol) with TbTR such that these quinone ligands are in the proximity of reduced trypanothione (Fig. 12). Similarly, both isoplumbagin and lawsone dock with the cysteine proteases rhodesain and TbCatB with the electrophilic carbons near the active-site cysteine residues (Fig. 13). *N. laevis* furanonaphthoquinones (α-lapachone derivatives) also dock with rhodesain in poses such that the nucleophilic Cys25 can undergo Michael addition to the quinone ring (Fig. 14). None of the furanonaphthoquinones docked near the trypanothione thiol groups in TbTR, however.

This *in-silico* investigation suggests that trypanosomal phytochemicals may target different protein targets. There are several caveats to these docking results: (a) many of the phytochemical agents may not be bioavailable due to limited solubility, membrane permeability, hydrolysis, or other metabolic decomposition; (b) tannins and other polyphenolics are promiscuous protein binding agents and are likely, therefore, not selective antitrypanosomal ligands; (c) the docking studies do not account for synergism in bioactivity of phytochemicals; (d) this current study does not address the binding of ligand to human homologous isozymes, which may also be targeted; (e) there are likely additional phytochemicals in each of the medicinal plants that have not been isolated or identified; and (f) there are likely additional trypanosomal proteins or other biochemical targets that have not yet been identified. Nevertheless, this *in-silico* molecular docking study has provided evidence for what phytochemical classes and structural manifolds are targeting particular trypanosomal protein targets and could provide the framework for synthetic modification of bioactive phytochemicals, *de novo* synthesis of structural motifs, and further phytochemical investigations.

Supporting Information

Table S1 Plants that have ethnopharmacological uses as antiprotozoal agents in West Africa.
(DOCX)

Table S2 Lowest-energy docking energies (kcal/mol) for *Acacia nilotica* phytochemicals with *Trypanosoma brucei* protein targets.
(DOCX)

Table S3 Lowest-energy docking energies (kcal/mol) for *Ageratum conyzoides* phytochemicals with *Trypanosoma brucei* protein targets.
(DOCX)

Table S4 Lowest-energy docking energies (kcal/mol) for *Annona senegalensis* phytochemicals with *Trypanosoma brucei* protein targets.
(DOCX)

Table S5 Lowest-energy docking energies (kcal/mol) for *Bridelia ferruginea* phytochemicals with *Trypanosoma brucei* protein targets.
(DOCX)

Table S6 Lowest-energy docking energies (kcal/mol) for *Carapa procera* phytochemicals with *Trypanosoma brucei* protein targets.
(DOCX)

Table S7 Lowest-energy docking energies (kcal/mol) for *Enantia chlorantha* phytochemicals with *Trypanosoma brucei* protein targets.
(DOCX)

Table S8 Lowest-energy docking energies (kcal/mol) for *Garcinia kola* phytochemicals with *Trypanosoma brucei* protein targets.
(DOCX)

Table S9 Lowest-energy docking energies (kcal/mol) for *Khaya ivorensis* and *Khaya senegalensis* phytochemicals with *Trypanosoma brucei* protein targets.
(DOCX)

Table S10 Lowest-energy docking energies (kcal/mol) for *Lawsonia inermis* phytochemicals with *Trypanosoma brucei* protein targets.
(DOCX)

Table S11 Lowest-energy docking energies (kcal/mol) for *Morinda lucida* phytochemicals with *Trypanosoma brucei* protein targets.
(DOCX)

Table S12 Lowest-energy docking energies (kcal/mol) for *Morinda morindoides* phytochemicals with *Trypanosoma brucei* protein targets.
(DOCX)

Table S13 Lowest-energy docking energies (kcal/mol) for *Nauclea latifolia* phytochemicals with *Trypanosoma brucei* protein targets.
(DOCX)

Table S14 Lowest-energy docking energies (kcal/mol) for *Newbouldia laevis* phytochemicals with *Trypanosoma brucei* protein targets.
(DOCX)

Table S15 Lowest-energy docking energies (kcal/mol) for *Physalis angulata* phytochemicals with *Trypanosoma brucei* protein targets.
(DOCX)

Table S16 Lowest-energy docking energies (kcal/mol) for *Picralima nitida* phytochemicals with *Trypanosoma brucei* protein targets.
(DOCX)

Table S17 Lowest-energy docking energies (kcal/mol) for *Prosopis africana* phytochemicals with *Trypanosoma brucei* protein targets.
(DOCX)

Table S18 Lowest-energy docking energies (kcal/mol) for *Rauwolfia vomitoria* phytochemicals with *Trypanosoma brucei* protein targets.
(DOCX)

Table S19 Lowest-energy docking energies (kcal/mol) for *Securidaca longipedunculata* phytochemicals with *Trypanosoma brucei* protein targets.
(DOCX)

Table S20 Lowest-energy docking energies (kcal/mol) for *Strychnos spinosa* phytochemicals with *Trypanosoma brucei* protein targets.
(DOCX)

Author Contributions

References

1. Vanhamme L, Paturiaux-Hanocq F, Poelvoorde P, Nolan DP, Lins L, et al. (2003) Apolipoprotein L-I is the trypanosomic lytic factor of human serum. Nature 422: 83–87.
2. Drugs for Neglected Diseases *initiative* (DND*i*). (2010) Fexinidazole (HAT). Available: http://www.dndi.org/portfolio/fexinidazole.html, Accessed 2012 Jan 12.
3. Torreele E, Trunz BB, Tweats D, Kaiser M, Brun R, et al. (2010) Fexinidazole – A new Oral nitroimidazole drug candidate entering clinical development for the treatment of sleeping sickness. PLoS Negl Trop Dis 4: e923
4. Simarro PP, Diarra A, Ruiz Postigo JA, Franco JR, Jannin JG (2011) The human African trypanosomiasis control and surveillance programme of the World Health Organization 2000–2009: The way forward. PLoS Negl Trop Dis 5: e1007
5. Fabeku OP, Akinsulire O (2008) The role of traditional medicine among the Yoruba of South-West Nigeria. In: A textbook of Medicinal Plants from Nigeria, Odugbemi T, ed. Lagos: University of Lagos Press. pp 43–54.
6. Jacobs RT, Nare B, Phillips MA (2011) State of the art in African trypanosome drug discovery. Curr Top Med Chem 11: 1255–1274.
7. Crowther GJ, Shanmugam D, Carmona SJ, Doyle MA, Hertz-Fowler C, et al. (2010) Identification of attractive drug targets in neglected disease pathogens using an *in silico* approach. PLoS Negl Trop Dis 4: e804
8. Schmidt TA, Khalid SA, Romanha AJ, Alves TMA, Biavatti MW, et al. (2012) The potential of secondary metabolites from plants as drugs or leads against protozoan neglected diseases – Part I. Curr Med Chem 19: 2128–2175.
9. Schmidt TA, Khalid SA, Romanha AJ, Alves TMA, Biavatti MW, et al. (2012) The potential of secondary metabolites from plants as drugs or leads against protozoan neglected diseases – Part II. Curr Med Chem 19: 2176–2228.
10. Lüscher A, Önal P, Schweingruber AM, Mäser P (2007) Adenosine kinase of *Trypanosoma brucei* and its role in susceptibility to adenosine antimetabolites. Antimicrob Agents Chemother 51: 3895–3901.
11. Dawson A, Gibellini F, Sienkiewicz N, Tulloch LB, Fyfe PK, et al. (2006) Structure and reactivity of *Trypanosoma brucei* pteridine reductase: Inhibition by the archetypal antifolate methotrexate. Mol Microbol 61: 1457–1468.
12. Gamarro F, Yu PL, Zhao J, Edman U, Greene PJ, et al. (1995) *Trypansoma brucei* dihydrofolate reductase-thymidylate synthase: Gene isolation and expression and characterization of the enzyme. Mol Biochem Parasitol 72: 11–22.
13. Krieger S, Schwarz W, Ariyanayagam MR, Fairlamb AH, Krauth-Siegel RL, et al. (2000) Trypanosomes lacking trypanothione reductase are avirulent and show increased sensitivity to oxidativestress. Mol Microbiol 35: 542–552.
14. Mackey ZB, O'Brien TC, Greenbaum DC, Blank RB, McKerrow JH (2004) A cathepsin B-like protease is required for host protein degradation in *Trypanosoma brucei*. J Biol Chem 279: 48426–48433.
15. Pallavi R, Roy N, Nageshan RK, Talukdar P, Pavithra SR, et al. (2010) Heat shock protein 90 as a drug target against protozoan infections. Biochemical characterization of hsp90 from *Plasmodium falciparum* and *Trypanosoma evansi* and evaluation of its inhibitor as a candidate drug. J Biol Chem 285: 37964–37975.
16. Lepesheva GI, Park HW, Hargrove TY, Vanhollebeke B, Wawrzak Z, et al. (2010) Crystal structures of *Trypanosoma brucei* sterol 14α-demethylase and implications for selective treatment of human infections. J Biol Chem 285: 1773–1780.
17. Parkin DW (1996) Purine-specific nucleoside *N*-ribohydrolase from *Trypanosoma brucei brucei*. J Biol Chem 271: 21713–21719.
18. Helfert S, Estévez AM, Bakker B, Michels P, Clayton C (2001) Roles of triosephosphate isomerase and aerobic metabolism in *Trypanosoma brucei*. Biochem J 357: 117–125.
19. Bosch J, Robien MA, Mehlin C, Boni E, Riechers A, et al. (2006) Using fragment cocktail crystallography to assist inhibitor design of *Trypanosoma brucei* nucleoside 2-deoxyribosyltransferase. J Med Chem 49: 5939–5946.
20. Shaw MP, Bond CS, Roper JR, Gourley DG, Ferguson MAJ, et al. (2003) High-resolution crystal structure of *Trypanosoma brucei* UDP-galactose 4′-epimerase: A potential target for structure-based development of novel trypanocides. Mol Biochem Parasitol 126: 173–180.
21. Grishin NV, Osterman AL, Brooks HB, Phillips MA, Goldsmith EJ (1999) X-ray structure of ornithine decarboxylase from *Trypanosoma brucei*: The native structure and the structure in complex with α-difluoromethylornithine. Biochemistry 38: 15174–15184.
22. Kerr ID, Lee JH, Farady CJ, Marion R, Rickert M, et al. (2009) Vinyl sulfones as antiparasitic agents and a structural basis for drug design. J Biol Chem 284: 25697–25703.
23. Marion R, Hansell E, Caffrey C, Roush WR, Brinin LS (2011) The high resolution crystal structure of rhodesain, the major cathepsin L protease from *T. brucei rhodesiense*, bound to inhibitor K11002. To be published, DOI:10.2210/pdb2p86/pdb.
24. Kuettel S, Greenwald J, Kostrewa D, Ahmed S, Scapozza L, et al. (2011) Crystal structures of *T. b. rhodesiense* adenosine kinase complexed with inhibitor and activator: Implications for catalysis and hyperactivation. PLoS Negl Trop Dis 5: e1164
25. Tulloch LB, Martini VP, Iulek J, Huggan JK, Lee JH, et al. (2010) Structure-based design of pteridine reductase inhibitors targeting African sleeping sickness and the leishmaniases. J Med Chem 53: 221–229.
26. Vanichtanankul J, Taweechai S, Yuvaniyama J, Vilaivan T, Chitnumsub P, et al. (2011) Trypanosomal dihydrofolate reductase reveals natural antifolate resistance. ACS Chem Biol 6: 905–911.
27. Patterson S, Alphey MS, Jones DC, Shanks EJ, Street IP, et al. (2011) Dihydroquinazolines as a novel class of *Trypanosoma brucei* trypanothione reductase inhibitors: Discovery, synthesis, and characterization of their binding mode by protein crystallography. J Med Chem 54: 6514–6530.
28. Kerr ID, Wu P, Marion-Tsukamaki R, Mackey ZB, Brinen LS (2010) Crystal structures of TbCatB and rhodesain, potential chemotherapeutic targets and major cysteine proteases of *Trypanosoma brucei*. PLoS Negl Trop Dis 4: e701
29. Wernimont AK, Hutchinson A, Sullivan H, Weadge J, Cossar D, et al. (2011) Crystal structure of the *N*-terminal domain of an HSP90 from *Trypanosoma brucei*, Tb10.26.1080 in the presence of a thienopyrimidine derivative. To be published, DOI:10.2210/pdb3omu/pdb.
30. Pizarro JC, Wernimont AK, Hutchinson A, Sullivan H, Chamberlain K, et al. (2011) Crystal structure of the *N*-terminal domain of an HSP90 from *Trypanosoma brucei*, Tb10.26.1080 in the presence of a benzamide derivative. To be published, DOI:10.2210/pdb3opd/pdb.
31. Vandemeulebroucke A, Minici C, Bruno I, Muzzolini L, Tornaghi P, et al. (2010) Structure and mechanism of the 6-oxopurine nucleosidase from *Trypanosoma brucei brucei*. Biochemistry 49: 8999–9010.
32. Noble MEM, Wierenga RK, Lambeir AM, Opperdoes FR, Thunnissen AMWH, et al. (1991) The adaptability of the active site of trypanosomal triosephosphate isomerase as observed in the crystal structures of three different complexes. Proteins Struct Funct Bioinf 10: 50–69.
33. Noble ME, Verlinde CL, Groendijk H, Kalk KH, Wierenga RK, et al. (1991) Crystallographic and molecular modeling studies on trypanosomal triosephosphate isomerase: A critical assessment of the predicted and observed structures of the complex with 2-phosphoglycerate. J Med Chem 34: 2709–2718.
34. Jackson LK, Brooks HB, Osterman AL, Goldsmith EJ, Phillips MA (2000) Altering the reaction specificity of eukaryotic ornithine decarboxylase. Biochemistry 39: 11247–11257.
35. Jackson LK, Goldsmith EJ, Phillips MA (2003) X-ray structure determination of *Trypanosoma brucei* ornithine decarboxylase bound to D-ornithine and to G418. J Biol Chem 278: 22037–22043.
36. Molegro Virtual Docker v 4.3 (2011) Aarhus, Denmark: Molegro ApS.
37. Thomsen R, Christensen MH (2006) MolDock: A new technique for high-accuracy molecular docking. J Med Chem 49: 3315–3321.
38. Spartan '08 for Windows, v 1.2 (2008) Irvine, California: Wavefunction, Inc.
39. Halgren TA (1996) Merck molecular force field. I. Basis, form, scope, parameterization, and performance of MMFF 94. J Comput Chem 17: 490–519.
40. Dictionary of Natural Products on DVD v 20:1 (2011) Boca Raton: Taylor and Francis.
41. Chaubal R, Pawar PV, Hebbalkar GD, Tungikar VB, Puranik VG, et al. (2005) Larvicidal activity of *Acacia nilotica* extracts and isolation of D-pinitol – a bioactive carbohydrate. Chem Biodivers 2: 684–688.
42. Eldeen IMS, Van Heerden FR, Van Staden J (2010) *In vitro* biological activities of nilioticane, a new bioactive cassane diterpene from the bark of *Acacia nilotica* subsp. *kraussiana*. J Ethnopharmacol 128: 555–560.
43. Singh R, Singh B, Singh S, Kumar N, Kumar S, et al. (2010) Umbelliferone – An antioxidant isolated from *Acacia nilotica* (L.) Willd. ex. Del. Food Chem 120: 825–830.
44. Maldini M, Montoro P, Hamed AI, Mahalel UA, Oleszek W, et al. (2011) Strong antioxidant phenolics from *Acacia nilotica*: Profiling by ESI-MS and qualitative–quantitative determination by LC-ESI-MS. J Pharmaceut Biomed Anal 56: 228–239.

45. Salem MM, Davidorf FH, Abdel-Rahman MH (2011) *In vitro* anti-uveal melanoma activity of phenolic compounds from the Egyptian medicinal plant *Acacia nilotica*. Fitoterapia 82: 1279–1284.

46. Ogbadoyi EO, Garba MH, Kabiru AY, Mann A, Okogun JI (2011) Therapeutic evaluation of *Acacia nilotica* (Linn) stem bark extract in experimental African trypanosomiasis. Int J Appl Res Nat Prod 4: 11–18.

47. Vyas AV, Mulchandani NB (1986) Polyoxygenated flavones from *Ageratum conyzoides*. Phytochemistry 25: 2625–2627.

48. González AG, Aguiar ZE, Grillo TA, Luis JG, Rivera A, et al. (1991) Methoxyflavones from *Ageratum conyzoides*. Phytochemistry 30: 1269–1271.

49. Nour AMM, Khalid SA, Kaiser M, Brun R, Abdalla WE, et al. (2010) The antiprotozoal activity of methylated flavonoids from *Ageratum conyzoides* L. J Ethnopharmacol 129: 127–130.

50. Sahpaz S, González MC, Hocquemiller R, Zafra-Polo MC, Cortes D (1996) Annonsenegalin and annogalene: Two cytotoxic mono-tetrahydrofuran acetogenins from *Annona senegalensis* and *Annona cherimolia*. Phytochemistry 42: 103–107.

51. Fatope MO, Audu OT, Takeda Y, Zeng L, Shi G, et al. (1996) Bioactive *ent*-kaurene diterpenoids from *Annona senegalensis*. J Nat Prod 59: 301–303.

52. Nkounkou-Loumpangou C, Gouollaly T, Mahmout Y, Elouma NAM, Ouamba JM, et al. (2010) Comparative study of the chemical composition of the essential oils from organs of *Annona senegalensis* Pers. *oulotricha* le Thomas subspecies (Annonaceae). Afr J Biotechnol 9: 887–891.

53. You M, Wickramaratne DBM, Silva GL, Chai H, Chagwedera TE, et al. (1995) (−)-Roemerine, an aporphine alkaloid from *Annona senegalensis* that reverses the multidrug-resistance phenotype with cultured cells. J Nat Prod 58: 598–604.

54. Waechter AI, Yaluff G, Inchausti A, Rojas de Arias A, Hocquemiller R, et al. (1998) Leishmanicidal and trypanocidal activities of acetogenins isolated from *Annona glauca*. Phytother Res 12: 541–544.

55. Ogbadoyi EO, Abdulganiy AO, Adama TZ, Okogun JI (2007) In vivo trypanocidal activity of *Annona senegalensis* Pers. leaf extract against *Trypanosoma brucei brucei*. J Ethnopharmacol 112: 85–89.

56. Ngueyem TA, Brusotti G, Caccialanza G, Vita Finzi P (2009) The genus *Bridelia*: A phytochemical and ethnopharmacological review. J Ethnopharmacol 124: 339–349.

57. Mulholland DA, Parel B, Coombes PH (2000) The chemistry of the Meliaceae and Ptaeroxylaceae of southern and eastern Africa and Madagascar. Curr Org Chem 4: 1011–1054.

58. Khalid SA, Friedrichsen GM, Kharazmi A, Theander TG, Olsen CE, et al. (1998) Limonoids from *Khaya senegalensis*. Phytochemistry 49: 1769–1772.

59. Bickii J, Njifutie N, Foyere JA, Basco LK, Ringwald P (2000) In vitro antimalarial activity of limonoids from *Khaya grandifoliola* C.D.C. (Meliaceae). J Ethnopharmacol 69: 27–33.

60. Hay AE, Ioset JR, Ahua KM, Diallo D, Brun R, et al. (2007) Limonoid orthoacetates and antiprotozoal compounds from the roots of *Pseudocedrela kotschyi*. J Nat Prod 70: 9–13.

61. Leite AC, Neto AP, Ambrozin ARP, Fernandes JB, Vieira PC, et al. (2010) Trypanocidal activity of flavonoids and limonoids isolated from Myrsinaceae and Meliaceae active plant extracts. Rev Bras Farmacog 20: 1–6.

62. Githua M, Hassanali A, Keriko J, Murilla G, Ndungu M, et al. (2010) New antitrypanosomal tetranortriterpenoids from *Azadirachta indica*. Afr J Trad Compl Alt Med 7: 207–213.

63. Wafo P, Nyasse B, Fontaine C, Sondengam BL (1999) Aporphine alkaloids from *Enantia chlorantha*. Fitoterapia 70: 157–160.

64. Bourdat-Deschamps M, Herrenknecht C, Akendengue B, Laurens A, Hocquemiller R (2004) Separation of protoberberine quaternary alkaloids from a crude extract of *Enantia chlorantha* by centrifugal partition chromatography. J Chromatogr A 1041: 143–152.

65. Wink M (2007) Molecular modes of action of cytotoxic alkaloids: From DNA intercalation, spindle poisoning, topoisomerase inhibition to apoptosis and multiple drug resistance. Alkaloids Chem Biol 64: 1–47.

66. Iwu M, Igboko O (1982) Flavonoids of *Garcinia kola*. J Nat Prod 45: 650–651.

67. Zhang B, Yang SP, Yin S, Zhang CR, Wu Y, et al. (2009) Limonoids from *Khaya ivorensis*. Phytochemistry 70: 1305–1308.

68. Olmo LRV, da Silva MFdGF, Fo ER, Vieira PC, Fernandes JB, et al. (1996) Rearranged limonoids from *Khaya senegalensis*. Phytochemistry 42: 831–837.

69. Olmo LRV, da Silva MFdGF, Fo ER, Vieira PC, Fernandes JB, et al. (1997) Limonoids from leaves of *Khaya senegalensis*. Phytochemistry 44: 1157–1161.

70. Abdelgaleil SAM, Okamura H, Iwagawa T, Sato A, Miyahara I, et al. (2001) Khayanolides, rearranged phragmalin limonoid antifeedants from *Khaya senegalensis*. Tetrahedron 57: 119–126.

71. Zhang H, Wang X, Chen F, Androulakis XM, Wargovich MJ (2007) Anticancer activity of limonoid from *Khaya senegalensis*. Phytother Res 21: 731–734.

72. Zhang H, Tan J, VanDerveer D, Wang X, Wargovich MJ, et al. (2009) Khayanolides from African mahogany *Khaya senegalensis* (Meliaceae): A revision. Phytochemistry 70: 294–299.

73. Adewunmi CO, Kayode Adesogan E (1984) Anthraquinones and oruwacin from *Morinda lucida* as possible agents in fasciolasis and schistosomiasis control. Fitoterapia 55: 259–263.

74. Sittie AA, Lemmich E, Olsen CE, Hviid L, Kharazmi A, et al. (1999) Structure-activity studies: *In vitro* antileishmanial and antimalarial activities of anthraquinones from *Morinda lucida*. Planta Med 65: 259–261.

75. Cimanga RK, Tona GL, Mesia GK, Kambu OK, Bakana DP, et al. (2006) Bioassay-guided isolation of antimalarial triterpenoid acids from the leaves of *Morinda lucida*. Pharmaceut Biol 44: 677–681.

76. Agbandje M, Jenkins TC, McKenna R, Reszka AP, Neidle S (1992) Anthracene-9,10-diones as potential anticancer agents. Synthesis, DNA-binding and biological studies on a series of 2,6-disubstituted derivatives. J Med Chem 35: 1418–1429.

77. Cimanga K, De Bruyne T, Lasure A, Li Q, Pieters L, et al. (1995) Flavonoid *O*-glycosides from the leaves of *Morinda morindoides*. Phytochemistry 38: 1301–1303.

78. Tamura S, Kubata BK, Syamsurizal, Itagaki S, Horii T, et al. (2010) New anti-malarial phenylpropanoid conjugated iridoids from *Morinda morindoides*. Bioorg Med Chem Lett 20: 1520–1523.

79. Manach C, Scalbert A, Morand C, Rémésy C, Jiménez L (2004) Polyphenols: Food sources and bioavailability. Am J Clin Nutr 79: 727–747.

80. Shigemori H, Kagata T, Ishiyama H, Morah F, Ohsaki A, et al. (2003) Neuclamides A–E, news monoterpene indole alkaloids from *Nauclea latifolia*. Chem Pharm Bull 51: 58–61.

81. Ngnokam D, Ayafor JF, Connolly JD, Nuzillard JM (2003) Neuclefolinine: A new alkaloid from the roots of *Nauclea latifolia*. Bull Chem Soc Ethiopia 17: 173–176.

82. Gafner S, Wolfender JL, Nianga M, Stoeckli-Evans H, Hostettmann K (1996) Antifungal and antibacterial naphthoquinones from *Newbouldia laevis* roots. Phytochemistry 42: 1315–1320.

83. Gormann R, Kaloga M, Li XC, Ferreira D, Bergenthal D, et al. (2003) Furanonaphthoquinones, atraric acid and a benzofuran from the stem barks of *Newbouldia laevis*. Phytochemistry 64: 583–587.

84. Adesanya SA, Nia R, Fontaine C, Païs M (1994) Pyrazole alkaloids from *Newbouldia laevis*. Phytochemistry 35: 1053–1055.

85. Aladesanmi AJ, Nia R, Nahrstedt A (1998) New pyrazole alkaloids from the root bark of *Newbouldia laevis*. Planta Med 64: 90–91.

86. Nagafuji S, Okabe H, Akahane H, Abe F (2004) Trypanocidal constituents in plants 4. Withanolides from the aerial parts of *Physalis angulata*. Biol Pharm Bull 27: 193–197.

87. Abe F, Nagafuji S, Okawa M, Kinjo J (2006) Trypanocidal constituents in plants 6. Minor withanolides from the aerial parts of *Physalis angulata*. Chem Pharm Bull 54: 1226–1228.

88. He QP, Ma L, Luo JY, He FY, Lou LG, et al. (2007) Cytotoxic withanolides from *Physalis angulata* L. Chem Biodivers 4: 443–449.

89. Kouam J, Mabeku LBK, Kuiate JR, Tiabou AT, Fomum ZT (2011) Antimicrobial glycosides and derivatives from roots of *Picralima nitida*. Int J Chem 3: 23–31.

90. Ratle G, Monseur X, Das BC, Yassi J, Khuong-Huu Q, et al. (1966) [Prosopine and prosopinine alkaloids of *Prosopis africana* (Guill and Perr) Taub. (preliminary note)]. Bul Soc Chim Fr 9: 2945–2947.

91. Sabri NN, Court WE (1978) Stem alkaloids of *Rauwolfia vomitoria*. Phytochemistry 17: 2023–2026.

92. Amer MM, Court WE (1980) Leaf alkaloids of *Rauwolfia vomitoria*. Phytochemistry 19: 1833–1836.

93. Marion Meyer JJ, Rakuambo NC, Hussein AA (2008) Novel xanthones from *Securidaca longipedunculata* with activity against erectile dysfunction. J Ethnopharmacol 119: 599–603.

94. Scandola M, Games DE, Costa C, Allegri G, Bertazzo A, et al. (1994) Structural study of alkaloids from *Securidaca longipedunculata* roots. II. Isolation and characterization by supercritical fluid chromatography/mass spectrometry. J Heterocycl Chem 31: 219–224.

95. Itoh A, Oya N, Kawaguchi E, Nishio S, Tanaka Y, et al. (2005) Secoiridoid glucosides from *Strychnos spinosa*. J Nat Prod 68: 1434–1436.

96. Hoet S, Pieters L, Muccioli GG, Habib-Jiwan JL, Opperdoes FR, et al. (2007) Antitrypanosomal activity of triterpenoids and sterols from the leaves of *Strychnos spinosa* and related compounds. J Nat Prod 70: 1360–1363.

97. Kerboeuf D, Riou M, Guégnard F (2008) Flavonoids and related compounds in parasitic disease control. Min Rev Med Chem 8: 116–128.

98. Pizzolatti MG, Mendes BG, Cunha A, Soldi C, Koga AH, et al. (2008) Trypanocidal activity of coumarins and styryl-2-pyrones from *Polygala sabulosa* A.W. Bennet (Polygalaceae). Rev Bras Farmacog 18: 177–182.

99. Rodgriquez AM, Enriz RD, Santagata LN, Jáuregui EA, Pestchanker MJ, et al. (1997) Structure-cytoprotective activity relationship of simple molecules containing an α,β-unsaturated carbonyl system. J Med Chem 40: 1827–1834.

100. Salas CO, Faundez M, Morello A, Diego Maya J, Tapia RA (2011) Natural and synthetic naphthoquinones active against *Trypanosoma cruzi*: An initial step towards new drugs for Chagas disease. Curr Med Chem 18: 144–161.

101. Salmon-Chemin L, Buisine E, Yardley V, Kohler S, Debreu MA, et al. (2001) 2- and 3-Substituted 1,4-naphthoquinone derivatives as subversive substrates of trypanothione reductase and lipoamide dehydrogenase from *Trypanosoma cruzi*: Synthesis and correlation between redox cycling activities and in vitro cytotoxicity. J Med Chem 44: 548–565.

102. De Molfetta FA, de Freitas RF, da Silva ABF, Montanari CA (2009) Docking and molecular dynamics simulation of quinone compounds with trypanocidal activity. J Mol Model 15: 1175–1184.